國立臺灣大學工學院環境工程學研究所

碩士論文

Graduate Institute of Environmental Engineering

College of Engineering

National Taiwan University

Master Thesis

# 利用過硫酸鹽氧化法處理電鍍製程產生之氰化物廢水

# Removal of cyanide from electroplating wastewater by persulfate oxidation process

王子軒

Zih-Syuan Wang

指導教授：林逸彬 博士

Advisor: Yi-Pin Lin Ph.D.

中華民國 111 年 8 月

August 2022

doi:10.6342/NTU202202427

# 國立臺灣大學碩士學位論文

# 口試委員會審定書

## 利用過硫酸鹽氧化法處理電鍍製程產生之氰化物廢水

## Removal of cyanide from electroplating wastewater by persulfate oxidation process

本論文係王子軒君(學號 R09541103)在國立臺灣大學環境工程學研究所完成之碩士學位論文，於民國 111 年 8 月 3 日承下列考試委員審查通過及口試及格，特此證明

論文審查委員：

林郁真博士
國立臺灣大學環境工程學研究所特聘教授

童心欣博士
國立臺灣大學環境工程學研究所教授

林逸彬博士
國立臺灣大學環境工程學研究所教授

黃鼎荃博士
朝陽科技大學環境工程與管理系
副教授兼系主任

指導教授：

所　　長：

# 誌謝

兩年的碩班時光，一轉眼就過去了，我學到了很多東西，也需要感謝很多人。最要感謝的是我的指導老師林逸彬教授，從一進實驗室開始，就帶著我們認識業界的老闆們，拓寬我們的視野，當我們碩二開始做研究、建築論文架構、操作實驗的時候，每次與老師的實驗成果報告，抑或是每週的共同會議，老師總是能夠給予我精準又實際的指導，找出我研究中的缺漏加以改善修正，此外，老師對於研究的邏輯思考更是要求，在學術研究上的嚴謹精神也是我需要向老師學習的地方。非常感謝老師這兩年的諄諄教誨，提升我在學術上的研究能力，並且培養我解決問題的能力。另外，還要特別感謝優勝奈米科技有限公司的許景翔總經理，讓我有機會接觸並進一步了解電鍍業氰化物這方面的研究，研究過程中則是不斷的支持與指點，給予我論文方向的一些發想與建議，非常感謝總經理的協助。

接著感謝儀秦學姊，學姊就像是我們實驗室中最強大的後盾，大大小小事情都是她一手包辦，當我遇到實驗卡關或是實驗結果闡釋相關疑惑時，學姊總是很細心、很有耐心的陪伴我一起解決，無私的與我分享她的經驗，指引我接下來的研究方向，讓我重拾研究的熱忱，還有在我剛進實驗室什麼都還不懂的時候，就要申請計畫，感謝學姊那時不厭其煩的教我計畫撰寫方式以及文獻整理引用格式等。再來要感謝我的實驗室夥伴筠茿、靖軒、昱騰，雖然我們的論文題目大不相同，共同在實驗室做實驗的時間也不一致，但只要是我們要一起完成的實驗室計畫，大家都會共同承擔分配，在實驗室偶爾巧遇，也會一同討論實驗設計與結果。還要感謝學弟妹文豪、聖翔、佳洪、明勳，協助完成實驗室的計畫，減輕我們一部分的壓力。

最後要感謝我的家人一路上的支持與陪伴，讓我能夠無後顧之憂的專注學業，成就現在更卓越的我。

doi:10.6342/NTU202202427

# 摘要

由於添加氰化物有助於增加電鍍金屬表面的光澤與美觀，因此被廣泛應用於電鍍製程，若未經妥善處理直接排放至環境，將會對生態及人類健康造成極大的危害。鹼性氯化法是一般常見的處理方法，但其可能會產生有毒的中間產物、過量消耗試劑、對金屬錯合氰化物去除效率低等缺點。本研究利用電鍍廢水中普遍存在的銅離子活化過二硫酸鹽，以降解水中氰化物，並透過調整不同水質參數，包含過二硫酸鹽(peroxydisulfate, PDS)、氰化物、銅離子濃度、陰離子、重金屬，探討其對過二硫酸鹽及氰化物降解效率的影響。此外，藉由副產物分析、自由基捕捉劑以及電子順磁共振實驗，確立相關的反應途徑及反應機制，最後，採集實廠電鍍廢水添加特定濃度的過二硫酸鹽，觀察氰化物降解效率並評估此方法的應用可行性。不同水質參數下的實驗結果顯示，當總氰化物濃度為 4 mM、過二硫酸鹽濃度為 10 mM、銅離子濃度為 1 mM 時，具有較好的氰化物降解效率，於反應 20 分鐘後，氰化物濃度降至 0.03 mM (相當於 0.83 mg/L $CN^-$)；添加多重陰離子的組別對於氰化物降解沒有顯著影響，而添加電鍍廢水常見的其他重金屬對氰化物降解效率的影響發現以下趨勢：$Cu^{2+} > Zn^{2+} > Fe^{2+} > Ni^{2+}$。在分析副產物的實驗結果，發現於 PDS/$CN^-$/$Cu^{2+}$的系統中，隨著氰化物的降解，氰酸鹽($OCN^-$)濃度有逐漸上升的趨勢；自由基捕捉劑以及電子順磁共振實驗結果顯示，於此活化系統中，明顯偵測到氫氧自由基與硫酸根自由基的存在，代表銅離子能成功活化 PDS 產生自由基促進氰化物降解。最後，於處理實際電鍍廢水的部分，添加 40 mM PDS 可於反應 20 分鐘內完全降解廢水中的氰化物。

關鍵字：氰化物、高級氧化、銅離子、過二硫酸鹽、氫氧自由基、硫酸根自由基



doi:10.6342/NTU202202427

# Abstract

Cyanide is widely used in electroplating process to ensure the smooth metal plating on the finished product surfaces. Alkaline chlorination process is commonly used to remove cyanide from electroplating wastewater. However, several drawbacks exist, including the formation of toxic intermediates, high consumption of chemical reagents, and low removal efficiency of metal-cyanide complexes. In this study, persulfate advanced oxidation process was explored for cyanide removal from electroplating wastewater. Peroxydisulfate (PDS) was activated by copper ion that is commonly present in electroplating wastewater to generate free radicals for cyanide removal. The influences of PDS concentration, cyanide concentration, copper ion concentration, common anions and heavy metals present in electroplating wastewater on cyanide removal and PDS consumption were investigated using batch experiments. The mechanism of cyanide oxidation was studied via the analysis of by-products, radical scavenging experiments, and electron paramagnetic resonance (EPR). Finally, real electroplating wastewater was collected from a local electroplating factory to the applicability of this process.

It was found that 99% removal of cyanide (4 mM) was achieved in the presence of 10 mM PDS and 1 mM $Cu^{2+}$ within 20 min in the PDS activation process. The presence of anions had no significant effects on cyanide removal. The ability of heavy metals on the activation of PDS for cyanide removal showed the following trend: $Cu^{2+}$ > $Zn^{2+}$ >



doi:10.6342/NTU202202427

$Fe^{2+} > Ni^{2+}$. For by-product analysis, cyanate was detected and its concentration gradually increased with cyanide concentration decreased as a function of time. The results of radical scavenging experiment and EPR showed that hydroxyl radical and sulfate radical were responsible for cyanide removal, indicating that copper ions can successfully activate PDS to generate free radicals to promote cyanide removal. For real electroplating wastewater, the addition of 40 mM PDS could completely remove cyanide in 20 min.

Keywords: cyanide, advanced oxidation process, copper ion, peroxydisulfate, hydroxyl radical, sulfate radical



doi:10.6342/NTU202202427

# Contents





doi:10.6342/NTU202202427

doi:10.6342/NTU202202427

# List of Figures





doi:10.6342/NTU202202427

doi:10.6342/NTU202202427

doi:10.6342/NTU202202427

# List of Tables





doi:10.6342/NTU202202427

# Chapter 1 Introduction

## 1.1 Background

Cyanide wastewater is generated from many industries such as electroplating, metallurgy, organic chemicals production, photographic, plastics, textiles, mining, etc. (Sarla et al., 2004; Kim et al., 2018). It can cause adverse effects on humans and aquatic life if discharged into the environments without proper treatments. According to the statistics of Taiwan Environmental Protection Administration (Taiwan EPA) Industrial Waste Report and Management System, electroplating industry is the major source of cyanide wastewater in Taiwan, generating about 4012 tons in 2020. Due to the high toxicity of cyanide, many countries have strict regulations on cyanide levels in water.

Cyanide treatment is generally classified into chemical treatment and biological treatment, both of which convert cyanide into less toxic compounds, usually cyanate ($OCN^-$). Among the chemical treatments, alkaline chlorination process is the most widely used process. Nevertheless, due to the formation of toxic cyanogen chlorine by-product and high amount of sludge generation, this process has been gradually replaced by other oxidation processes (Teixeira et al., 2013; Botz et al., 2016).

Advanced Oxidation Processes (AOPs), including $H_2O_2$, $O_3$, $KMnO_4$, and persulfate have been applied for the treatment of toxic contaminants (Chen et al., 2014; Kim et al.,



doi:10.6342/NTU202202427

2018; Nava et al., 2003; Ordiales et al., 2015; Moussavi et al., 2018; Chegini et al., 2020). Free radicals such as hydroxyl radicals or sulfate radicals can be generated in AOPs for effective removal of contaminants. Peroxydisulfate (PDS) is a strong oxidant. It is stable in ambient conditions and requires activation, such as thermal, photolytic, sonolytic, alkaline, and metal ions to generates radicals (Wang et al., 2018). PDS has been widely used in the treatment of organic compounds. However, there is no report on the activation of PDS by metal ions that are already present in the electroplating wastewater for cyanide oxidation.

## 1.2 Research objectives

The objectives of this study are:

1. To investigate the removal of cyanide by PDS activated by metal ions present in the electroplating wastewater.
2. To investigate the influences of operating parameters on cyanide removal by PDS AOP.
3. To study the reaction mechanism of cyanide removal.
4. To evaluate the efficiency and suitability of this system for the treatment of real electroplating wastewater.



doi:10.6342/NTU202202427

# Chapter 2 Literature Reviews

## 2.1 Electroplating wastewater

The electroplating process involves three major steps, including pre-treatment (grinding, polishing, degreasing, and rust removing), electroplating process and post-treatment (coating, plating, and drying). Based on the statics of Taiwan EPA in 2020, the wastewater generated from plating bath solutions and spent stripping and cleaning bath solutions from electroplating operations were 1363 tons and 2648 tons, respectively.

Cyanide has been used in the electroplating process to ensure the homogeneous and smooth plating of metals on materials (Zhang et al., 2015; Pérez-Cid et al., 2020). The composition of electroplating wastewater is complicated and may contain abrasives, polishing agents, degreasing agents, acids, and various plating compounds such as copper sulfate, nickel sulfate, cuprous cyanide, and potassium cyanide. General characteristic of electroplating wastewater is shown in Table 1 (EPA, 1979; Industrial Development Bureau, 2002; Kim et al., 2003; Moussavi et al., 2018; 李依釗, 2016):



doi:10.6342/NTU202202427

Table 1. Properties of electroplating wastewater.

| Constituents | Concentration (mg/L) |
|---|---|
| Cyanide | 0.5-230 |
| COD | 52-580 |
| SS | 0.15-9970 |
| Ni | 0.019-2954 |
| Cu | 0.032-272.5 |
| Zn | 0.112-252 |
| Fe | 0.41-1482 |

## 2.2 Toxicity of cyanide

Cyanide exists in two forms in wastewater: simple cyanide such as HCN, KCN and NaCN and metal-cyanide complexes including strong cyanide complexes of Au, Co, Fe and weak and moderately strong cyanide complexes of Ag, Cd, Cu, Ni, Zn (Parga et al., 2003; Botz et al., 2016). The toxicity of different cyanide species depends on how easily $CN^-$ is released, as indicated in Table 2 (Adams, 2013; Johnson, 2015).

Exposure to high levels of cyanide can cause rapid breathing, tremors, neurological effects, weight loss, and even death (Dash et al., 2009; Gurbuz et al., 2009). Due to the high toxicity of cyanide, many countries have strict regulations on the cyanide content in water, as shown in Table 3.



doi:10.6342/NTU202202427

Table 2. Relative toxicity and stability of cyanide (Adams, 2013; Johnson, 2015).

| Group | Species | Relative toxicity | Stability constant (log $\beta_n$) |
|---|---|---|---|
| Simple cyanide | HCN, NaCN, KCN, $CN^-$ | High | - |
| Weak and moderately strong complexes | $Cu(CN)_2^-$ | Intermediate | 16.3 |
| | $Cd(CN)_4^{2-}$ | | 17.9 |
| | $Zn(CN)_4^{3-}$ | | 19.6 |
| | $Ag(CN)_2^-$ | | 20.5 |
| | $Ni(CN)_4^{2-}$ | | 30.2 |
| Strong complexes | $Au(CN)_2^-$ | Low | 38.5 |
| | $Fe(CN)_6^{3-}$ | | 43.6 |
| | $Co(CN)_6^{3-}$ | | 64.0 |
| Cyanide-related species | $SCN^-$ | Low | |
| | $OCN^-$ | Low | |
| | CNCl | High | |



doi:10.6342/NTU202202427

Table 3. Water quality standards for cyanide.

| Country/organization | Standard |
|---|---|
| WHO | 0.07 mg/L (for drinking water) |
| US | 0.2 mg/L (for drinking water) |
| Singapore | 0.1 mg/L (for effluents) |
| Germany | 0.2 mg/L (for electroplating processes effluents) |
| China | 0.3 mg/L (for electroplating industry effluents) |
| Swaziland | 0.5 mg/L (for effluents) |
| Japan | 1.0 mg/L (for effluents) |
| Korea | 1.0 mg/L (for effluents) |
| Taiwan | 1.0 mg/L (for electroplating industry effluents) |

## 2.3 Cyanide treatment

Conventionally, alkaline chlorination process is the most widely used treatment process for cyanide removal (Figure 1) (NIEA, 2011).



doi:10.6342/NTU202202427

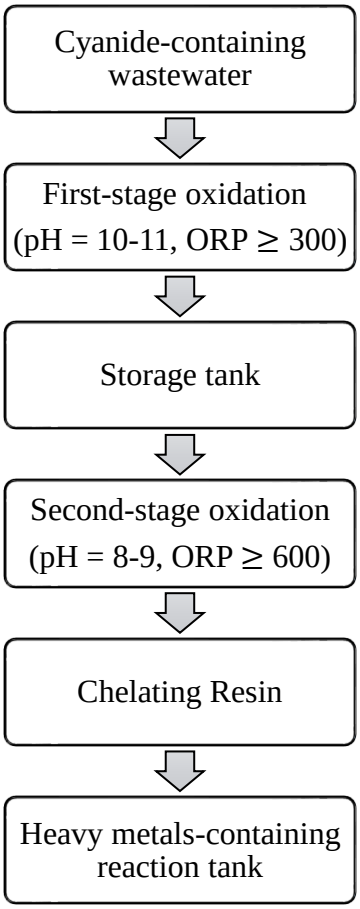


Figure 1. Alkaline chlorination process (NIEA, 2011).

Two steps are involved in the process: the first step is to convert cyanide to cyanate, and the second step is to oxidize cyanate to nitrogen gas. The corresponding reactions are shown as follows:

$$OCl^- + CN^- \rightarrow OCN^- + Cl^- \quad (1)$$

$$2OCN^- + 3OCl^- + H_2O \rightarrow N_2 + 3Cl^- + 2HCO_3^- \quad (2)$$

However, this process has some drawbacks such as toxic by-products (CNCl) formation and inefficiency for removing metal-cyanide complexes, etc. (Kim et al., 2003; Yang et



doi:10.6342/NTU202202427

al., 2020). For those reasons, AOPs are considered to be an attractive alternative for cyanide removal. Common AOP treatments involve the use of $SO_2$/air, $H_2O_2$, $O_3$, $KMnO_4$, and persulfate. $SO_2$/air was patented and marked by the International Nickel Company (INCO) in the 1980s for the oxidation of cyanide ions to cyanate using $SO_2$ and air over a soluble copper catalyst (Devuyst et al., 1989; Branch, 1993). Hydrogen peroxide treatment follows a similar detoxification mechanism as $SO_2$/air. In this process, $H_2O_2$ is used as the oxidant and copper ion is also required as a catalyst. It has been reported that as the concentration of $H_2O_2$ and $Cu^{2+}$ increases, the removal efficiency of cyanide increases. Sarla et al. (2004) reported that 90% of cyanide ($[CN^-]_0$ = 100 mg/L) removal after 24 h at pH 10.0 with a $H_2O_2$ dose of 88.2 mM and a complete degradation of cyanide ($[CN^-]_0$ = 100 mg/L) in 9 min with a $H_2O_2$ dose of 88.2 mM and a $Cu^{2+}$ catalyst concentration of 75 mg/L. Kim et al. (2018) reported that almost 99% cyanide ($[CN^-]_0$ = 100 mg/L) was removed after 60 min at pH 11.0 in the presence of 2.5% $H_2O_2$ and 95% cyanide was removed after 20 min in the presence of 0.05% $H_2O_2$ and 50 mg/L $Cu^{2+}$. Additionally, several studies have investigated the efficiency of a combination of ozone and hydrogen peroxide on cyanide removal (Kim et al., 2003; Pueyo et al., 2016). Some studies use potassium permanganate as an oxidant to remove cyanide in wastewater due to its strong oxidation ability and relatively low toxicity (Adachi et al., 1991; Ordiales et al., 2015). Peroxymonosulfate ($H_2SO_5$, PMS) is a powerful oxidant ($e^o_H$ = 1.84 V), and it



doi:10.6342/NTU202202427

was prepared by $H_2SO_4$ and $H_2O_2$. Teixeira et al. (2013) reported that the reduction of cyanide from 400 mg/L to 1.0 mg/L after 10 min of reaction under the following condition: $H_2SO_5$:$CN^-$ = 4.5:1 and pH = 9. Chegini et al. (2020) revealed that cyanide ($[CN^-]_0$ = 50 mg/L) can be completely degraded within 4 min in the UV/$O_3$/PMS process.

## 2.4 Activation of peroxydisulfate

Conventional AOPs rely on the generation of hydroxyl radicals, a non-selective oxidant with a redox potential of 2.8V to remove the target contaminants. Compared with hydroxyl radicals, sulfate radicals are highly selective with a redox potential of 2.5-3.1 (Guerra-Rodríguez et al., 2018). Sulfate radicals can be generated through the activation of peroxymonosulfate (PMS) or peroxydisulfate (PDS). Activation methods include heat, UV, alkaline, electrochemical, metal ions, and activated carbon have been reported (Anipsitakis et al., 2004; Devi et al., 2016; Matzek et al., 2016). In terms of cost, PDS ($0.74 per kg) is much cheaper than PMS ($2.20 per kg) and $H_2O_2$ ($1.52 per kg), making PDS attractive for real application (Anipsitakis et al., 2003; Lau et al., 2007). Several studies have demonstrated the feasibility of using thermal (Wei et al., 2022), metal ions (Budaev et al., 2015), metal oxide (Behnami et al., 2021), and UV-activated persulfate oxidation (Moussavi et al., 2018; Castilla-Acevedo et al., 2020; Satizabal-Gómez et al., 2021) for the removal of cyanide from contaminated soils or wastewater. According to



doi:10.6342/NTU202202427

the above studies, cyanide treatment requires additional equipment or reagents, which will increase the cost of treatment. Although copper ions mostly exist in electroplating wastewater, most studies consider that the copper activation of persulfate is a low reaction rate process on organic pollutants treatment (Ding et al., 2022). Chegini et al. (2020) found that copper ions can improve cyanide removal in PMS activation in an UV/ozone process, but the copper activation of PDS on cyanide removal is still unclear. Otherwise, those studies did not use electron paramagnetic resonance (EPR) to confirm the presence of radicals, and most proposed that hydroxyl radicals were the dominant oxidative species in the process and the contribution of sulfate radicals was ignored.

Persulfate can be activated through electron transfer by metals or metal oxides such as iron, copper, silver, and other metals to form sulfate radicals as shown in Figure 2 (Wang et al., 2018). Metals and metal oxides can be divided into homogeneous and heterogeneous according to their existence form. Among the homogeneous metal ions, $Ag^+$ was the most efficient catalyst for activating PDS (Anipsitakis et al., 2004). Although homogeneous metal ions can directly react with PDS to decrease the mass transfer effects, they are greatly affected by the pH and water composition and require the secondary treatment of residual metal ions in wastewater (Wang et al., 2018). Since copper ions mostly exist in electroplating wastewater for base plating and intermediate plating, the mechanism of copper-catalyst PDS system is mainly studied. In activation of PDS by



doi:10.6342/NTU202202427

$Cu^{2+}$, $SO_4^-$ ·, OH · and $Cu^{3+}$ are usually identified as possible reactive species, generating by direct one-electron transfer from $Cu^{2+}$ to PDS. The oxidation of $Cu^{2+}$ by PDS is favorable in thermodynamics due to the redox potentials of PDS(2.01 V) and $Cu^{3+}/Cu^{2+}$(1.57 V) (Popova et al., 2003). Although the formed $Cu^{3+}$ may act as a strong oxidant for oxidizing pollutants and regenerate $Cu^{2+}$, it tends to combine with ligands to stabilize at neutral to alkaline pH condition (Chen et al., 2019; Ding et al., 2022).

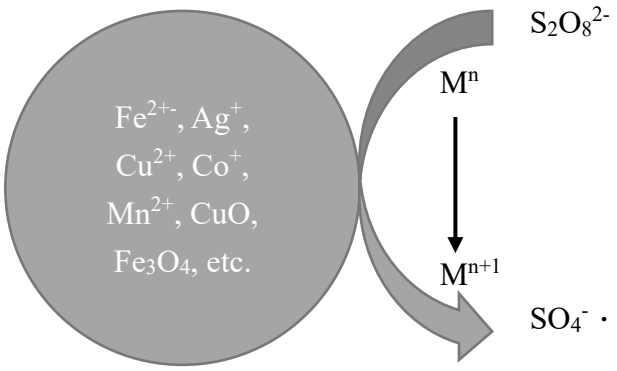


Figure 2. Mechanism of metal and metal oxide activation of PDS (Wang et al., 2018).

Furthermore, adjusting the pH value to alkaline condition is essential for cyanide removal by PDS oxidation. Furman et al. (2010) proposed that PDS is first hydrolyzed leading to the formation of hydroperoxide ($HO_2^-$) and sulfate ($SO_4^{2-}$). The hydroperoxide then reduces another PDS to generate $SO_4^-$ ·, sulfate and superoxide ($O_2^-$ ·) (Equation ( 3 ), ( 4 )). Sulfate radicals can react with hydroxide ions to generate hydroxyl radicals (OH ·) under alkaline condition (Equation ( 5 )). Finally, cyanide ions react with hydroxyl radicals and sulfate radicals to form cyanate ($OCN^-$) and other by-products including



doi:10.6342/NTU202202427

ammonia, nitrogen gas, nitrite, nitrate, etc. (Buxton et al., 1988; Kim et al., 2003; Furman et al., 2010; Guan et al., 2011; Cui et al., 2012; Moussavi et al., 2016; Wei et al., 2022).

$$S_2O_8^{2-} + 2H_2O \xrightarrow{OH-} HO_2^- + 2SO_4^{2-} + 3H^+ \quad (3)$$

$$HO_2^- + S_2O_8^{2-} \rightarrow SO_4^- \cdot + SO_4^{2-} + H^+ + O_2^- \cdot \quad (4)$$

$$SO_4^- \cdot + OH^- \rightarrow SO_4^{2-} + OH \cdot \quad (5)$$

$$CN^- + OH \cdot \rightarrow C(OH)=N \cdot \quad (6)$$

$$C(OH)=N \cdot + OH \cdot \rightarrow OCN^- + H_2O \quad (7)$$

$$OCN^- + H_2O + 2OH \cdot \rightarrow CO_3^{2-} + NH_4^+ \quad (8)$$

$$OCN^- + 3OH \cdot \rightarrow CO_3^{2-} + 0.5\ N_2 + H_2O + H^+ \quad (9)$$

$$OCN^- + 6OH \cdot \rightarrow NO_2^- + CO_3^{2-} + 2H^+ + 2H_2O \quad (10)$$

$$NO_2^- + 2OH \cdot \rightarrow NO_3^- + H_2O \quad (11)$$

$$CN^- + 2SO_4^- \cdot + H_2O \rightarrow OCN^- + 2SO_4^{2-} + 2H^+ \quad (12)$$



doi:10.6342/NTU202202427

# Chapter 3 Materials and Methods

## 3.1 Research framework

The research flowchart of this study is shown in Figure 3. First, the effect of different operating parameters on cyanide removal by the PDS process using synthetic solutions was evaluated. Then, the optimal conditions were selected for subsequent tests. By-product analysis and radical quenching experiments were conducted to investigate the reaction mechanism in the $S_2O_8^{2-}/Cu^{2+}$ process. Lastly, real electroplating cyanide wastewater was used to assess the applicability of the process.

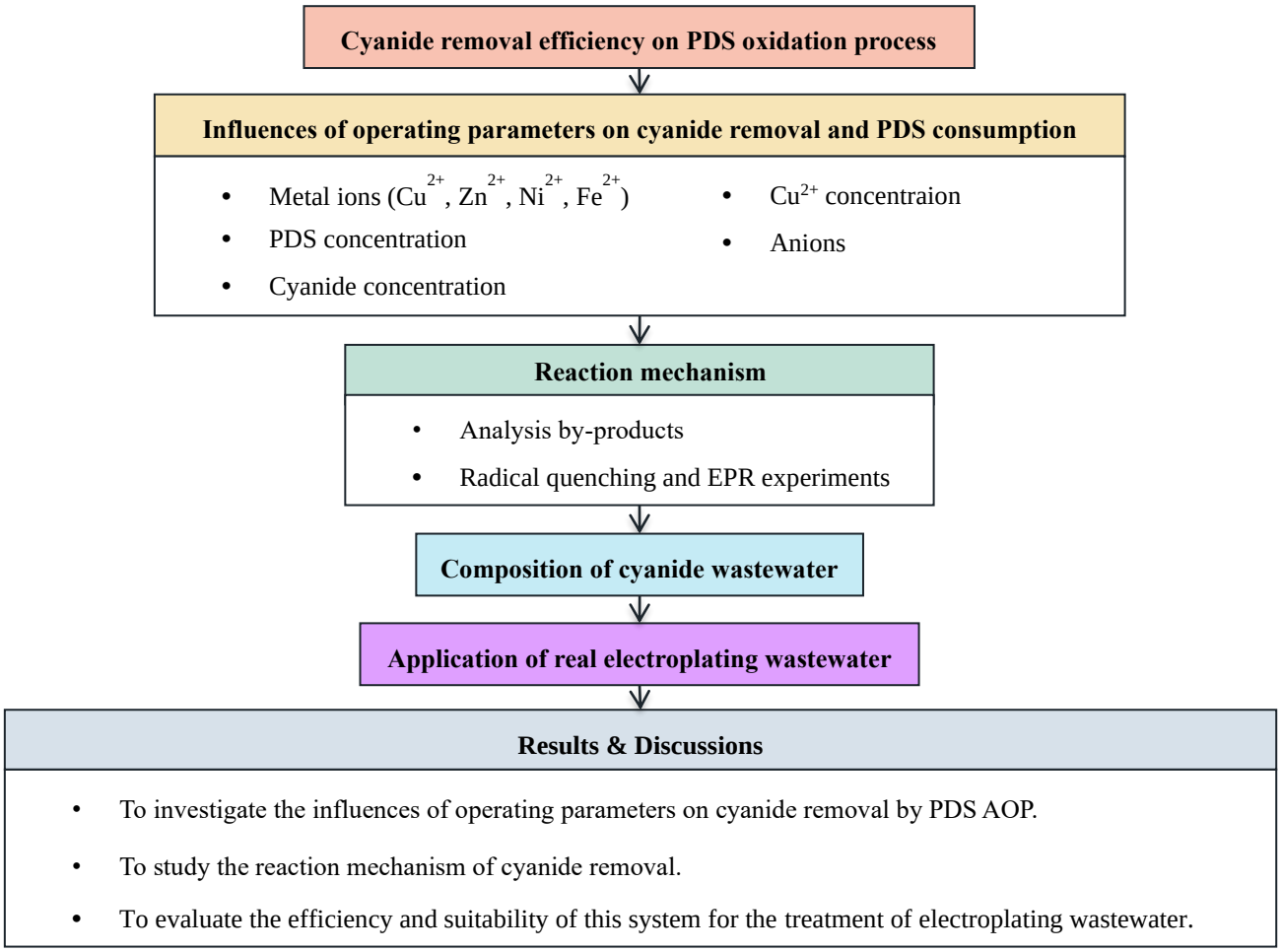


Figure 3. Research flowchart of overall experiments.



doi:10.6342/NTU202202427

## 3.2 Chemical and reagents

Potassium cyanide (KCN) and sodium acetate ($CH_3COONa$) were purchased from Acros Organics, USA. Chloramine-T, barbituric acid and monopotassium phosphate ($KH_2PO_4$) were purchased from Alfa Aesar, USA. Sulfuric acid ($H_2SO_4$, 95-97%), hydrochloric acid (HCl, 37%), acetic acid ($CH_3COOH$, 100%), sodium hydroxide (NaOH), sodium tetraborate ($Na_2B_4O_7 \cdot 10H_2O$), ferrous sulfate heptahydrate ($FeSO_4 \cdot 7H_2O$), sodium persulfate ($Na_2S_2O_8$), sodium fluoride (NaF), and sodium benzoate ($NaC_6H_5CO_2$) were purchased from Honeywell Fluka, USA. N,N-diethyl-p-phenylenediamine (DPD), cupric sulfate pentahydrate ($CuSO_4 \cdot 5H_2O$), nickel dichloride hexahydrate ($NiCl_2 \cdot 6H_2O$), ethylenediaminetetraacetic acid disodium salt dihydrate (EDTA-salt, $C_{10}H_{14}N_2Na_2O_8 \cdot H_2O$), sodium nitrate ($NaNO_3$), sodium nitrite ($NaNO_2$), potassium sulfate ($K_2SO_4$), ammonium chloride ($NH_4Cl$), methanol ($CH_3OH$, hypergrade for LC-MS), ethanol ($C_2H_5OH$, 99.9%), and 4-chlorobenzoic acid ($C_7H_5O_2Cl$, pCBA) were purchased from Merck, Germany. Magnesium chloride hexahydrate ($MgCl_2 \cdot 6H_2O$), zinc sulfate heptahydrate ($ZnSO_4 \cdot 7H_2O$), sulfamic acid ($NH_2SO_3H$), pyridine ($C_5H_5N$, 99.8%), sodium dihydrogen phosphate ($NaH_2PO_4$), and trisodium citrate ($Na_3C_6H_5O_7$) were purchased from Sigma-Aldrich, USA. Sodium hydrogen phosphate ($Na_2HPO_4$), sodium hypochlorite (NaOCl, 5%), sodium chloride (NaCl), and phosphoric acid ($H_3PO_4$, 85-87%) were purchased from J.T. Baker, USA. Phenol ($C_6H_6O$, ≥89%) and sodium



doi:10.6342/NTU202202427

nitroprusside ($C_5FeN_6Na_2O$) were purchased from Nacalai Tesque, Japan. 5,5-Dimethyl-1-Pyrroline-N-Oxide (DMPO) was purchased from Dojindo, Japan. All chemicals were analytical grade, and solutions were prepared with deionized water generated from PURELAB Classical system, ELGA (R = 18.2 MΩ · cm).

## 3.3 Experimental procedures

Experiments were performed in a 500 ml batch reactor at 25 ± 1 ℃. Synthetic solutions were freshly prepared by diluting a given amount of KCN with the pH maintained at around 10.0 using 0.03 M borate buffer to avoid the release of $HCN_{(g)}$ during the experiment. 1 M persulfate stock solutions and 50 g/L $CuSO_4{\cdot}5H_2O$ solutions were added into the solution to achieve the desired persulfate and copper ion concentrations under magnetic bar stirring. All experiments were carried out in duplicate. Control experiments without the addition of copper ions and under neutral conditions were also conducted.

The effects of persulfate concentration (1 to 10 mM), cyanide concentration (2 to 12 mM), copper ion concentration (0.1 to 4 mM), presence of anions (5000 mg/L of $F^-$, $Cl^-$, $NO_2^-$, $NO_3^-$, $PO_4^{3-}$, and $SO_4^{2-}$), and co-presence of metal ions (1 mM of $Ni^{2+}$, $Zn^{2+}$ and $Fe^{2+}$) on cyanide removal and persulfate consumption were investigated. The concentrations of anions and metal ions used were based on the properties of



doi:10.6342/NTU202202427

electroplating wastewater. After initiating the experiments, the samples were taken at desired time intervals from the reactor and divided into two tubes for persulfate and cyanide measurements, respectively. Before adding the samples to the tubes, reducing agent (sodium thiosulfate, $Na_2S_2O_3 \cdot 5H_2O$) was added to quench residual persulfate and EDTA was added to complex with copper ions. The schematic of the batch experiment is shown in Figure 4 and the experimental conditions employed is shown in Table 4.

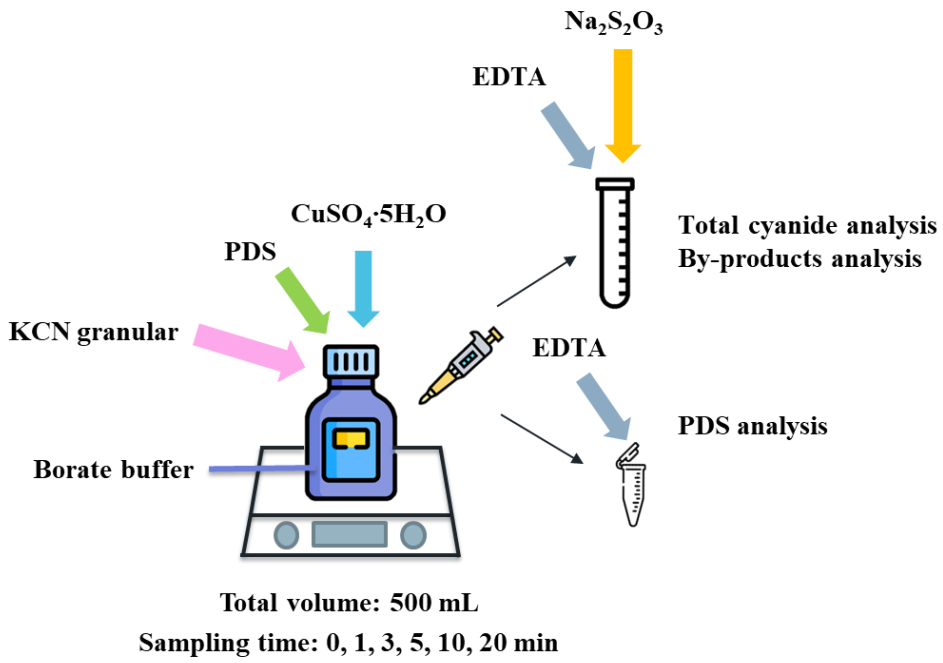


Figure 4. The schematic diagram of batch experiment.



doi:10.6342/NTU202202427

Table 4. The experimental conditions employed for optimization of different operating parameters.

| | PDS dosage | Cyanide concentration | $Cu^{2+}$ concentration |
|---|---|---|---|
| $[CN^-]_0$ (mM) | 4 | 2, 4, 8, 12 | 4 |
| $[PDS]_0$ (mM) | 0, 1, 2, 5, 10 | 10 | 10 |
| $[Cu^{2+}]_0$ (mM) | 1 | 1 | 0, 0.1, 0.25, 0.5, 1, 2, 4 |

In order to explore the pathway of cyanide oxidation, possible by-products including cyanate ($OCN^-$), nitrate, nitrite, and ammonia were measured. For this part, experiments with and without the addition of copper ions were conducted.

The contribution of different radicals on the removal of cyanide was investigated using radical quenching and electron paramagnetic resonance (EPR) experiments. Specifically, methanol and 4-chlorobenzoic acid (pCBA) were used to quench hydroxyl radicals, and benzoic acid (BA) was used to quench hydroxyl radicals and sulfate radicals. Details of each radical scavenging and EPR experiments are shown in Table 5 and Table 6, respectively. Lastly, real electroplating wastewater was used to evaluate the applicability of this process in the industry.

Table 5. The value of parameters in radical scavenging experiments.

| | Methanol | pCBA | BA |
|---|---|---|---|
| $[CN^-]_0$ (mM) | 4 | 0, 4 | 0, 4 |
| $[PDS]_0$ (mM) | 10 | | |
| $[Cu^{2+}]_0$ (mM) | 1 | | |
| [MeOH] (M) | 2.5, 5, 10 | - | - |
| [pCBA] or [BA] (μM) | - | 100 | 100 |



doi:10.6342/NTU202202427

Table 6. Different groups of EPR experiments.

| Total volume: 50 ml<br>Sampling time: 1 min<br>Condition: [DMPO] = 1 M, [Borate buffer] = 0.03 M,<br>[$CN^-$] = 4 mM, [$Cu^{2+}$] = 1 mM, [PDS] = 10 mM | |
|---|---|
| G1 | DMPO + Borate buffer |
| G2 | DMPO + Borate buffer + $CN^-$ |
| G3 | DMPO + Borate buffer + $Cu^{2+}$ |
| G4 | DMPO + Borate buffer + PDS |
| G5 | DMPO + Borate buffer + $CN^-$ + $Cu^{2+}$ |
| G6 | DMPO + Borate buffer + $CN^-$ + PDS |
| G7 | DMPO + Borate buffer + PDS + $Cu^{2+}$ |
| G8 | DMPO + Borate buffer + PDS + $CN^-$ + $Cu^{2+}$ |

## 3.4 Analytic methods

Total cyanide concentration was determined by 4500-$CN^-$ colorimetric method after distillation (APHA et al., 2017). EDTA and $Na_2S_2O_3$ were added to terminate the cyanide oxidation reaction and stored by adding NaOH to raise the pH to 12-12.5. During distillation, hydrogen cyanide (HCN) gas was released from the acidified sample by using 1+1 $H_2SO_4$, heated with rapid boiling for at least 1 hour, and collected in 1 M NaOH scrubbing solution. The distillation apparatus is shown in Figure 5. Then, 2.5 ml of distilled sample was mixed with 0.1 ml of acetate buffer and 0.2 ml of the chloramine-T solution to convert cyanide to CNCl under pH<8. Finally, 0.5 ml of pyridine-barbituric acid reagent was added to react with CNCl to form purple color, diluted to 5 ml with distilled water, and measured the absorbance at 578 nm after standing for 8 min.



doi:10.6342/NTU202202427

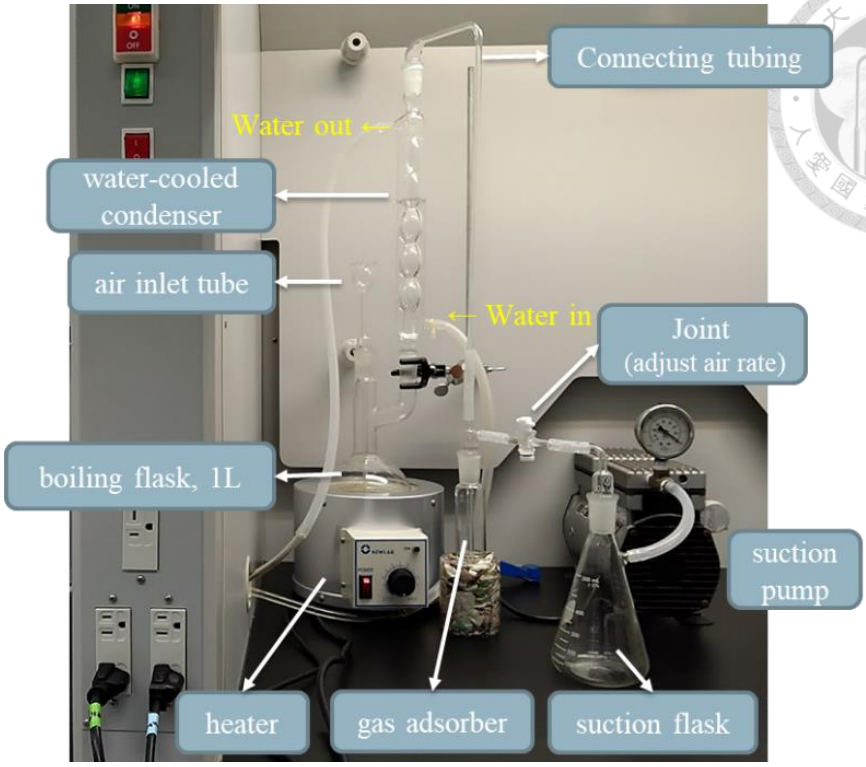


Figure 5. The distillation apparatus for cyanide determination.

Persulfate concentration was determined by the spectrophotometric method using N,N-diethyl-p-phenylenediamine (DPD), in which persulfate oxidizes DPD to form pink color (Gokulakrishnan et al., 2016). EDTA was also added to terminate cyanide oxidation reaction. 2 ml of sample was mixed with 1 ml of phosphate buffer and 0.2 ml of 2.5 mM DPD solution and diluted to 10 ml with distilled water. After standing for 10 min, the absorbance at 551 nm was measured. The concentration of persulfate was calculated by Equation ( 13 ) :

$$[PDS] = \frac{\Delta A}{\varepsilon \times b} \frac{V_{final}}{V_{sample}} \qquad (13)$$

where $\Delta A$ represents the absorbance at 551 nm after blank correction; $\varepsilon$ is molar



doi:10.6342/NTU202202427

extinction coefficient, 21000 $M^{-1}$ $cm^{-1}$; b is path length of optical cell, 1 cm; $V_{final}$ and $V_{sample}$ are the final volume (10 ml) after addition of all reagents and volume of the original sample (2 ml), respectively.

Cyanate concentration was determined by measuring the difference in ammonia content using the phenate method before and after cyanate hydrolysis (APHA et al., 2017). 0 ml of the sample was acidified by adding 0.1 ml of 1+1 $H_2SO_4$ to hydrolyze $OCN^-$ to $NH_4^+$. The sample was then heated at 95ºC for 30 min. 0.25 ml of 10 M NaOH was added to the sample to convert $NH_4^+$ to $NH_3$, followed by the ammonia measurement. Ammonia concentration was determined by the 4500-$NH_3$ phenate method (APHA et al., 2017). Under the catalysis of sodium nitroprusside, the reaction of ammonia in the sample with hypochlorite and phenol will generate blue indophenol. 5 ml of the sample was mixed with 0.2 ml of phenol solution, 0.2 ml of sodium nitroprusside solution, and 0.5 ml of oxidizing solution. After standing for 1 hour, the absorbance at 640 nm was measured. The UV absorbance was measured using the UV-vis spectrophotometer (Shimadzu, UV-1800).

Anion concentrations were determined by the ion chromatography (IC, Dionex ICS-1100) and heavy metal concentrations were determined by the inductively coupled plasma optical emission spectrometry (ICP-OES, Agilent 700 series). The concentration of pCBA and BA were determined by the high performance liquid chromatography (HPLC



doi:10.6342/NTU202202427

primaide, HITACHI) system equipped with a ZOBAX XDB-C18 column (4.6 × 150 mm, 5 μm pore size, Agilent Technologies) and a variable wavelength detector (1430 Diode Array Detector, HITACHI). The mobile phase used a mixture of methanol and 10 mM $H_3PO_4$ and the detection wavelength for pCBA and BA were 240 and 227 nm, respectively. Detailed conditions are described in Table 7 (Cheng et al., 2022).

In the EPR experiments, 0.875 ml of sample was mixed with 0.125 ml of DMPO for 30 seconds and analyzed by an EPR system (Bruker, EMX-plus, USA) with the following condition: center field = 3500 G, sweep width = 120 G, microwave frequency = 9.84 GHz, power = 31.88 mW, modulation amplitude = 1.25 G, modulation frequency = 100 kHz, and sweep time = 60 s. The surface morphology and element composition of precipitate formed after the reaction was analyzed using the field-emission scanning electron microscope coupled with energy dispersive X-ray analysis (FESEM-EDS) (JEOL, JSM-7600F). The pH value was measured by a calibrated pH meter (Suntex, SP-2100).



doi:10.6342/NTU202202427

Table 7. HPLC mobile phase condition used for the determination of pCBA and BA.

| Compounds | Isocratic mobile phase | | | Flow rate (ml/min) |
|---|---|---|---|---|
| | Time (min) | Methanol (%) | 10 mM $H_3PO_4$ (%) | |
| pCBA | 0 | 40 | 60 | 0.6 |
| BA | 0 | 10 | 90 | 1 |
| | 2 | 10 | 90 | |
| | 8 | 60 | 40 | |
| | 11 | 60 | 40 | |
| | 13 | 10 | 90 | |



doi:10.6342/NTU202202427

# Chapter 4 Results & Discussions

## 4.1 Influences of metal ions, PDS concentration, cyanide concentration, $Cu^{2+}$ concentration, and anions on PDS consumption and cyanide removal

PDS can be activated by metal ions, such as copper, silver, cobalt and ferric ions to generate radicals to remove pollutants (Wang et al., 2018; Zheng et al., 2022). Many metal ions present in cyanide-containing electroplating wastewater and they may activate PDS for the removal of cyanide. Common metal ions seen in the electroplating wastewater including $Cu^{2+}$, $Ni^{2+}$, $Fe^{2+}$ and $Zn^{2+}$ were evaluated individually for their abilities to activate PDS for cyanide removal in synthetic wastewater.

The influences of the above-mentioned metal ions on PDS consumption and cyanide removal are shown in Figure 6. The experiments were conducted with an initial pH of 10.2, an initial PDS concentration of 10 mM and an initial cyanide concentration of 4 mM in the presence of borate buffer and 1 mM of each of the metal ions. The final pH decreased in the end of the experiments, ranging from 9.8-10.1, as shown in Table 8. In the absence of any metal ions, 2.3 mM (21%) PDS was consumed and 1.2 mM (31%) cyanide was removed likely due to the alkaline activation of PDS. With the addition of 1 mM of $Ni^{2+}$, $Fe^{2+}$, $Zn^{2+}$ and $Cu^{2+}$, the PDS consumption was 11.7%, 23.1%, 33.6%, and 67.1%, and the cyanide removal was 10.0%, 34.3%, 53.8% and 99.3%, respectively. The



doi:10.6342/NTU202202427

addition of $Ni^{2+}$ seemed to inhibit the activation of PDS and the removal of cyanide. The addition of $Fe^{2+}$ did not accelerate the consumption of PDS nor the removal of cyanide. The addition of $Zn^{2+}$ and $Cu^{2+}$, on the other hand, accelerated the PDS consumption and cyanide removal. To sum up, the cyanide removal in the presence of different metal ions showed the following trend: $Cu^{2+} > Zn^{2+} > Fe^{2+} > Ni^{2+}$. One interesting observation was that blue and red precipitates were found in the end of the experiments with the addition of $Cu^{2+}$ and $Fe^{2+}$, respectively, suggesting that the concentrations of $Cu^{2+}$ and $Fe^{2+}$ in the experimental solutions would decrease as the reaction proceeded. In conclusion, $Cu^{2+}$ is the most effective in the activation of PDS. Following experiments were conducted to specifically examine the activation of PDS by $Cu^{2+}$ for cyanide removal.



doi:10.6342/NTU202202427

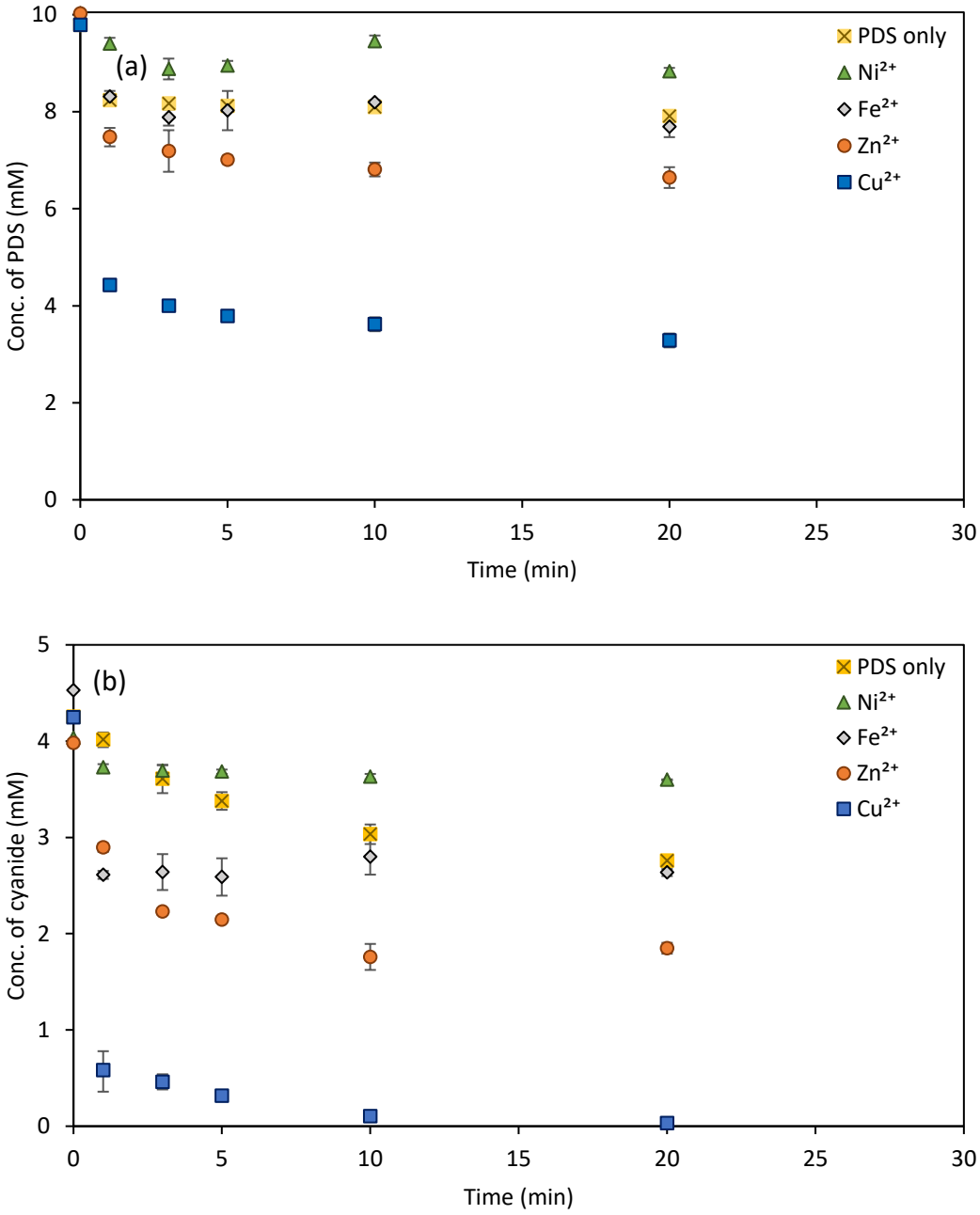


Figure 6. Influence of metal ions on (a) PDS consumption and (b) cyanide removal. (Experimental condition: initial pH = 10.2, [$CN^-$] = 4 mM, borate buffer = 0.03 M, [PDS] = 10 mM, [$Ni^{2+}$, $Fe^{2+}$, $Zn^{2+}$, $Cu^{2+}$] = 1 mM)

Table 8. Initial and final pH for experiments using different metal ions.

| | PDS only | $Ni^{2+}$ | $Fe^{2+}$ | $Zn^{2+}$ | $Cu^{2+}$ |
|---|---|---|---|---|---|
| Initial pH | 10.2 | | | | |
| Final pH | 10.1 | 10.1 | 10.1 | 10.1 | 9.8 |



doi:10.6342/NTU202202427

The influence of PDS concentration on PDS consumption and cyanide removal is shown in Figure 7. The experiments were conducted with an initial pH of 10.1 and initial cyanide concentration of 4 mM in the presence of borate buffer and 1 mM of $Cu^{2+}$. The final pH did not change significantly, ranging from 10.0 to 9.7, as shown in Table 9. In control experiment without PDS, cyanide concentration decreased slightly to 3.6 mM. It was speculated that $Cu^{2+}$ can form complex with cyanide ion and decrease the concentration of total cyanide measured through the distillation process. In the presence of PDS, PDS was almost completely consumed and 35.0% and 55.3% of cyanide were removed after 1 min when [PDS] = 1 and 2 mM ([PDS]/[$CN^-$] = 0.25 and 0.5), respectively. The results suggested that the reaction was very fast and these two PDS concentrations were insufficient to completely remove cyanide. When [PDS] increased to 5 and 10 mM ([PDS]/[$CN^-$] = 1.25 and 2.5), the PDS concentration decreased with time and 92.8% and 99.3% of cyanide were removed in the end of the experiments, indicating that the molar ratio of [PDS]/[$CN^-$] should be greater than 1 for efficient cyanide removal. The cyanide concentration dropped to 0.03 mM (0.83 mg/L) after 20 min in the presence of 10 mM PDS, which met the Taiwan EPA discharging water quality standard (1 mg/L) for electroplating industry.



doi:10.6342/NTU202202427

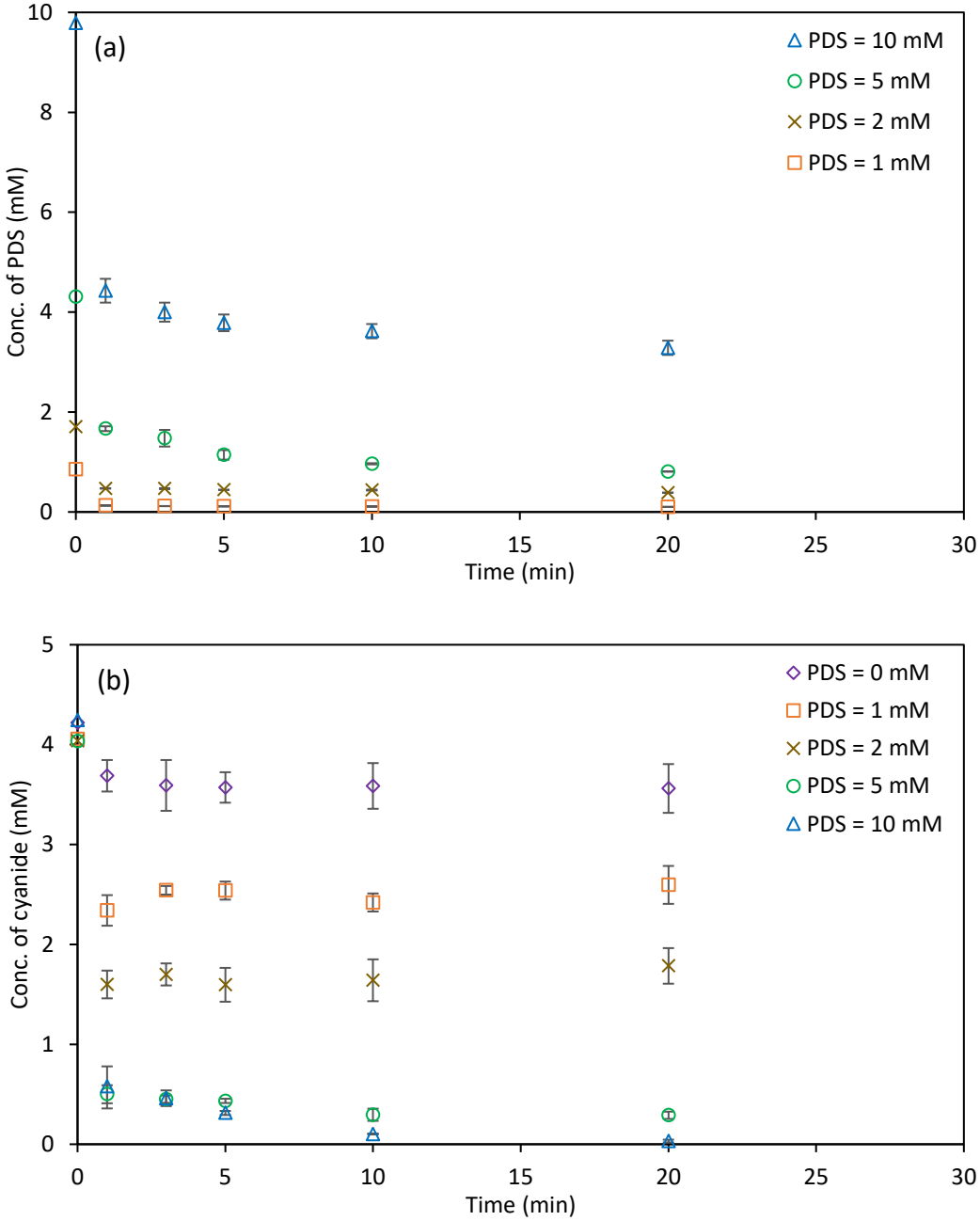


Figure 7. Influence of PDS concentration on (a) PDS consumption and (b) cyanide removal. (Experimental condition: initial pH = 10.1, $[CN^-]$ = 4 mM, borate buffer = 0.03 M, $[Cu^{2+}]$ = 1 mM)

Table 9. Initial and final pH for experiments using different PDS concentrations.

| **Initial conc. of PDS (mM)** | 0 | 1 | 2 | 5 | 10 |
|---|---|---|---|---|---|
| Initial pH | 10.1 | | | | |
| Final pH | 10.0 | 10.0 | 10.0 | 9.8 | 9.7 |



doi:10.6342/NTU202202427

The influence of cyanide concentration on PDS consumption and cyanide removal is shown in Figure 8. The experiments were conducted with an initial pH of 10.2 and initial PDS concentration of 10 mM in the presence of borate buffer and 1 mM of $Cu^{2+}$. The final pH did not change significantly, ranging from 9.9-10.0 as shown in Table 10. In general, the consumption of PDS was faster at a higher cyanide concentration after the reaction was initiated. However, PDS consumption was almost the same (68.1%) at 20 min when the cyanide concentration was 4-12 mM (molar ratio of [PDS]/[$CN^-$] was 0.83 to 2.5), in which 89.1%-99.3% of cyanide were removed. It was speculated that the concentration of $Cu^{2+}$ was insufficient to activate PDS to remove all cyanide.



doi:10.6342/NTU202202427

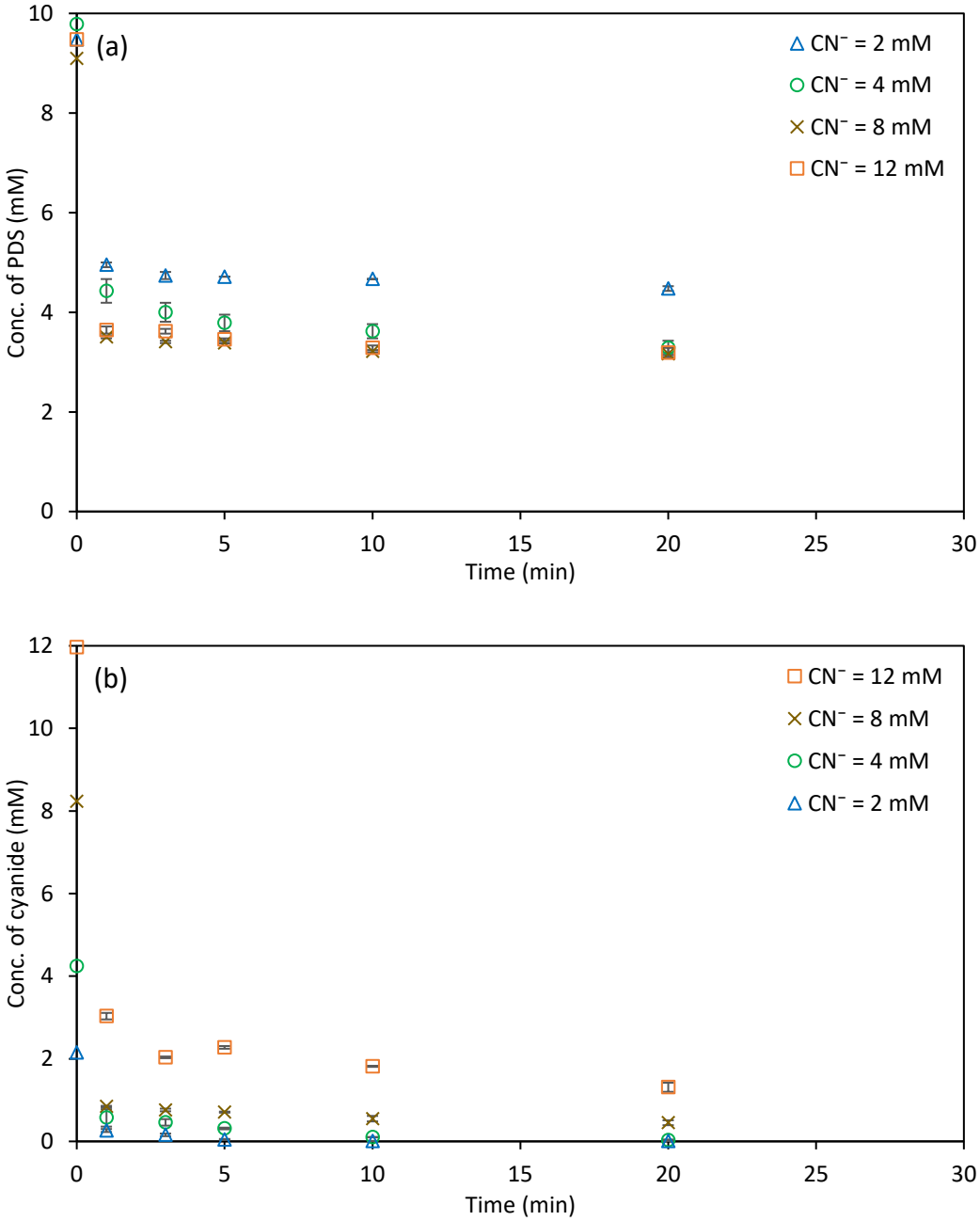


Figure 8. Influence of cyanide concentration on (a) PDS consumption and (b) cyanide removal. (Experimental condition: initial pH = 10.2, [PDS] = 10 mM, borate buffer = 0.03 M, $[Cu^{2+}]$ = 1 mM)

Table 10. Initial and final pH for experiments using different cyanide concentrations.

| **Initial conc. of cyanide (mM)** | 2 | 4 | 8 | 12 |
|---|---|---|---|---|
| Initial pH | 10.2 | | | |
| Final pH | 9.9 | 9.8 | 10.0 | 10.0 |



doi:10.6342/NTU202202427

The influence of $Cu^{2+}$ concentration on PDS consumption and cyanide removal is shown in Figure 9. The experiments were carried out with an initial pH of 10.2, an initial PDS concentration of 10 mM and an initial cyanide concentration of 4 mM in the presence of borate buffer and 0-4 mM of $Cu^{2+}$. The final pH did not change significantly, ranging from 9.8-10.1, as shown in Table 11. In control experiment without $Cu^{2+}$, about 30% of cyanide was removed, indicating that PDS could be activated by the alkaline pH and contributed to the cyanide removal. A higher $Cu^{2+}$ concentration resulted in a greater PDS consumption and a greater cyanide removal. When the concentration of $Cu^{2+}$ was 0.1 mM, 32.6% of PDS was consumed and 69.3% of cyanide was removed, indicating that $Cu^{2+}$ concentration was not enough to activate sufficient PDS for complete cyanide removal. When the concentration of $Cu^{2+}$ increased to 0.5 mM and 1 mM, 91.5% and 99.3% of cyanide was removed, respectively. No significant difference was found in the consumption of PDS and the removal of cyanide when [$Cu^{2+}$] was 1, 2, and 4 mM, suggesting that the optimal concentration of $Cu^{2+}$ was 1 mM when [PDS] = 10 mM and [$CN^-$] = 4 mM. This condition was selected for further study.



doi:10.6342/NTU202202427

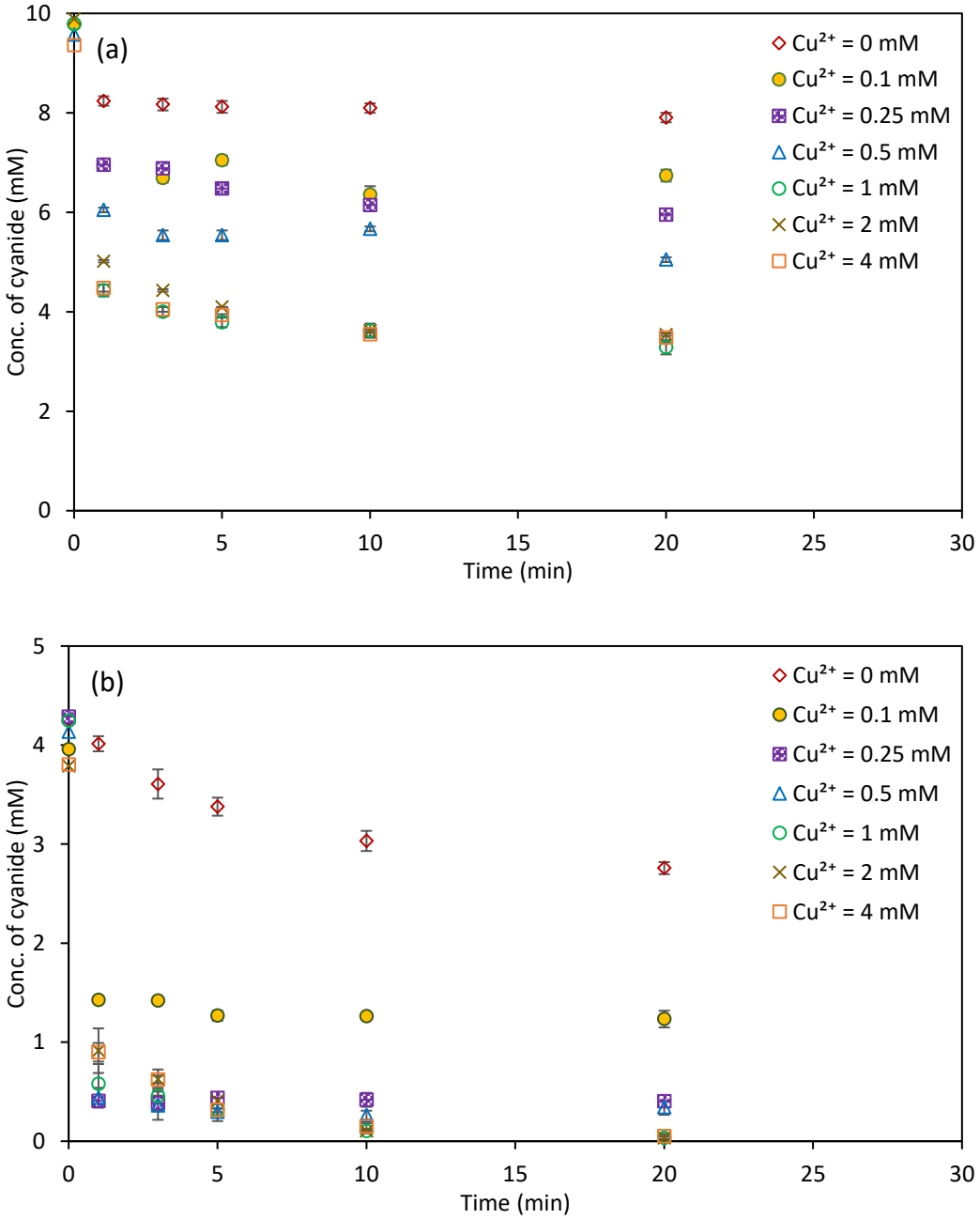


Figure 9. Influence of $Cu^{2+}$ concentration on (a) PDS consumption and (b) cyanide removal. (Experimental condition: initial pH = 10.2, $[CN^-]$ = 4 mM, borate buffer = 0.03 M, [PDS] = 10 mM)

Table 11. Initial and final pH for experiments using different $Cu^{2+}$ concentrations.

| **Initial conc. of $Cu^{2+}$ (mM)** | 0 | 0.1 | 0.25 | 0.5 | 1 | 2 | 4 |
|---|---|---|---|---|---|---|---|
| Initial pH | 10.2 | | | | | | |
| Final pH | 10.1 | 10.1 | 10.0 | 9.9 | 9.8 | 9.8 | 9.8 |



doi:10.6342/NTU202202427

The influence of different anions on PDS consumption and cyanide removal is shown in Figure 10. In order to simulate the composition of real electroplating wastewater, the experiment was carried out with the addition of 5000 mg/L of $F^-$, $Cl^-$, $NO_2^-$, $NO_3^-$, $SO_4^{2-}$, and $PO_4^{3-}$ into the synthetic solution. The initial pH was 10.4 and the final pH slightly decreased to 10.1 in the end of the experiment. Compared to the result without anions, the addition of anions consumed 10.7% more of PDS but had no effect on cyanide removal, indicating that the presence of anions would not affect the removal of cyanide.



doi:10.6342/NTU202202427

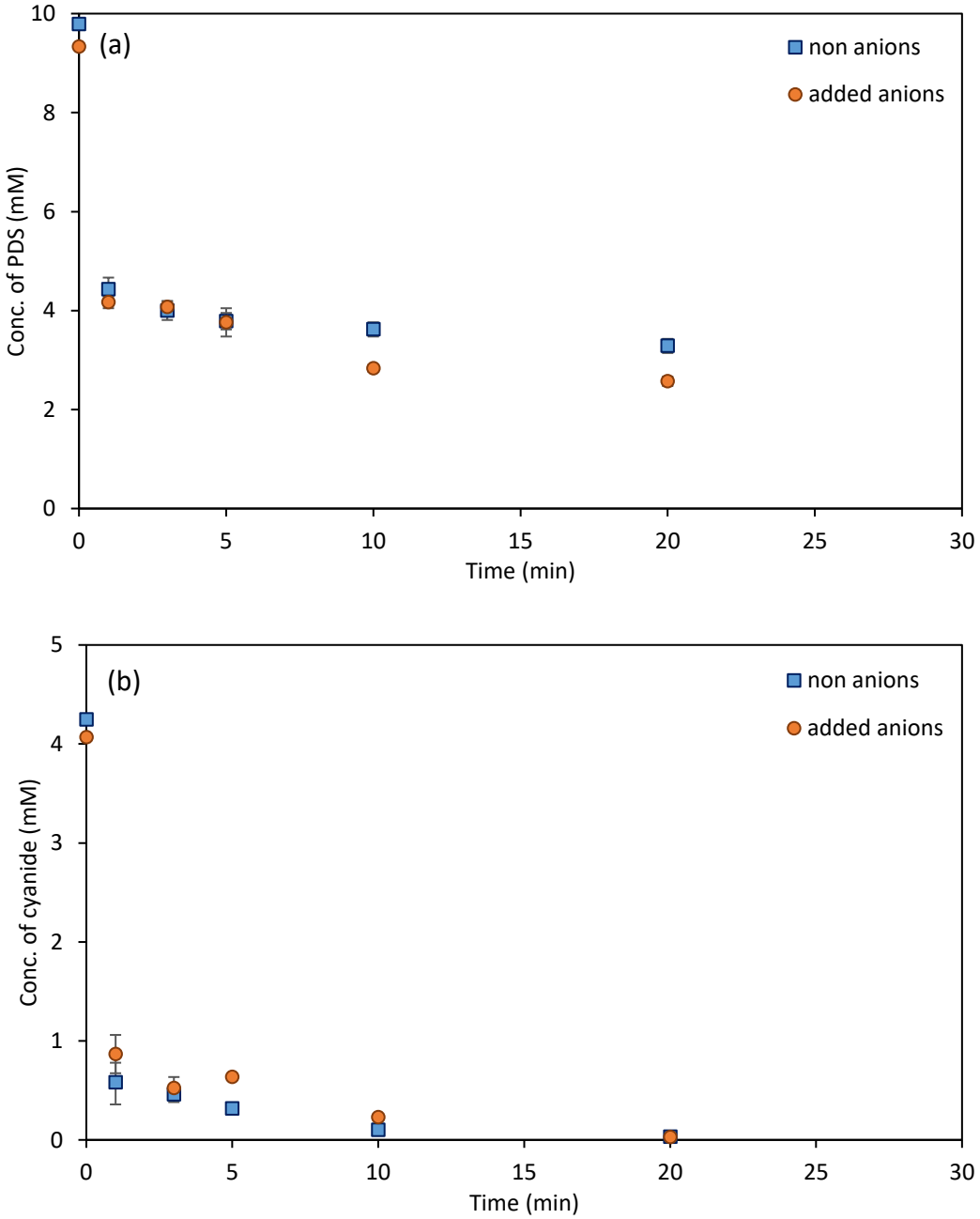


Figure 10. Influence of anions on (a) PDS consumption and (b) cyanide removal. (Experimental condition: initial pH = 10.4, $[CN^-]$ = 4 mM, borate buffer = 0.03 M, [PDS] = 10 mM, $[Cu^{2+}]$ = 1 mM, anions: 5000 mg/L of $F^-$, $Cl^-$, $NO_2^-$, $NO_3^-$, $SO_4^{2-}$, $PO_4^{3-}$)



doi:10.6342/NTU202202427

## 4.2 Cyanide removal at near neutral pH

Since PDS can be activated under alkaline condition to generate free radicals, experiment at near neutral pH were conducted to clarify the contribution of alkaline activation of PDS to cyanide oxidation. The experiment was carried out with the initial pH of 7.5 in the presence of phosphate buffer and the final pH decreased slightly due to addition of PDS or $Cu^{2+}$, ranging from 7.0-7.4, as shown in Table 12. Figure 11 shows that the concentration of PDS did not change significantly in the absence of $Cu^{2+}$ and the concentration of cyanide decreased slightly over time. There was a difference between near neutral and alkaline conditions on cyanide removal in the PDS/$CN^-$ group. 30% of cyanide removal was observed at pH 10.2 (Figure 9), but only 15.9% of cyanide removal was found at near neutral pH, indicating that alkaline activation of PDS had about 15% contribution to cyanide removal. In the presence of 1 mM of $Cu^{2+}$, 34.1% of PDS consumption and 91.3% of cyanide removal were found after 20 min, suggesting that PDS can be activated by $Cu^{2+}$ at near neutral condition, but this removal efficiency of cyanide was slightly lower than that at alkaline pH, which 99.3% of cyanide removal was observed (Figure 9). It should be noted that at near neutral pH, the formation of toxic HCN (pKa = 9.3) and its evaporation is a concern. Most cyanide wastewater facilities add base to cyanide wastewater to increase the pH to alkaline conditions to avoid the formation of HCN in their operations.



doi:10.6342/NTU202202427

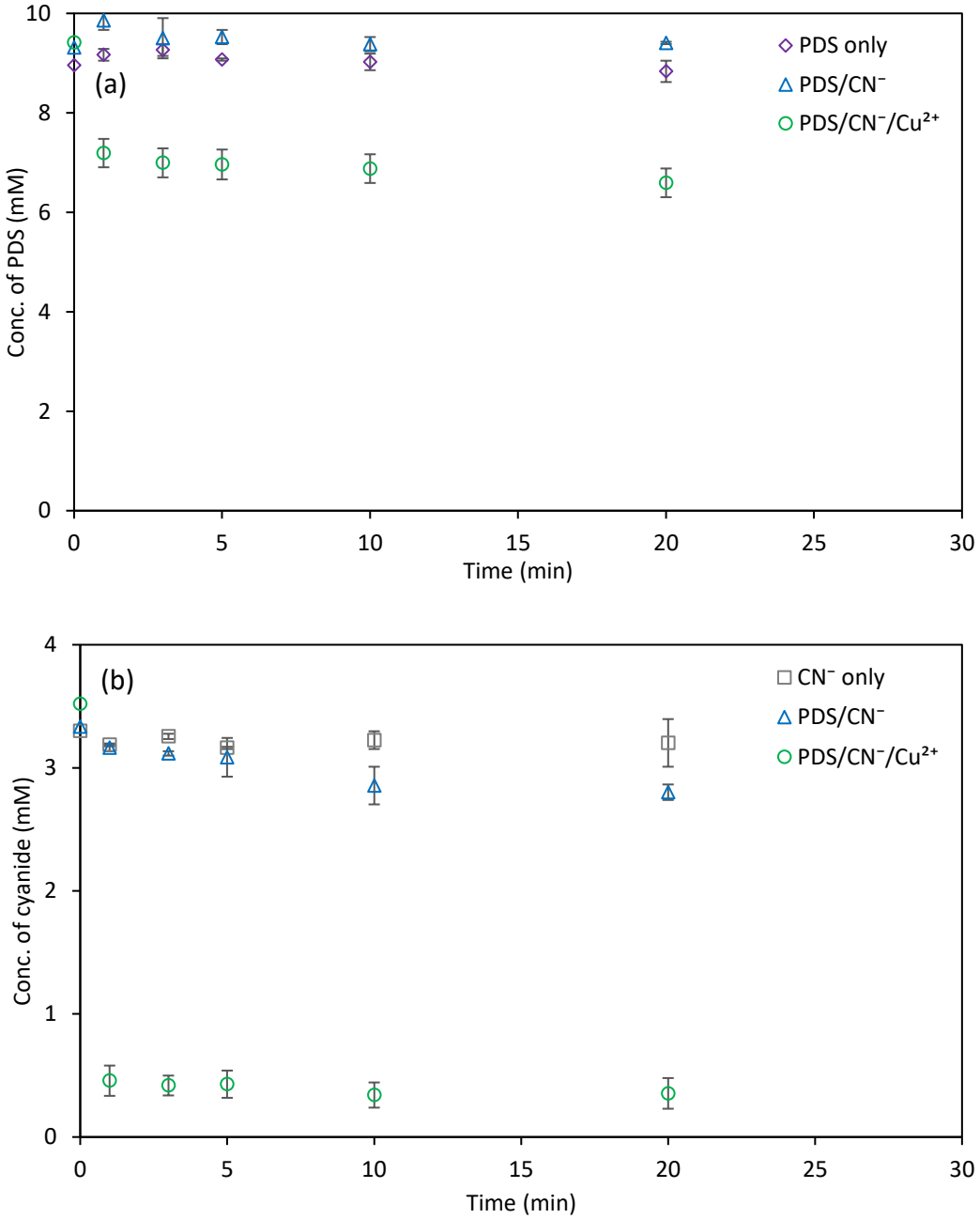


Figure 11. Control experiment in PDS oxidation process at near neutral pH (a) PDS consumption and (b) cyanide removal. (Experimental condition: initial pH = 7.5, $[CN^-]$ = 4 mM, [PDS] = 10 mM, $[Cu^{2+}]$ = 1 mM)

Table 12. Initial and final pH for control experiments at near neutral pH.

| | PDS only | $CN^-$ only | PDS/$CN^-$ | PDS/$CN^-$/$Cu^{2+}$ |
|---|---|---|---|---|
| Initial pH | 7.5 | | | |
| Final pH | 7.1 | 7.4 | 7.3 | 7.0 |



doi:10.6342/NTU202202427

## 4.3 Radical scavenging and radical probe experiments

Radical scavenging experiments were carried out to investigate the reaction mechanism and confirm the contribution of free radicals in cyanide removal. Methanol was employed as a scavenger for OH · and $SO_4^-$ · . The second-order rate constants of methanol with OH · and $SO_4^-$ · are $9.7\times10^8$ $M^{-1}s^{-1}$ and $1.1\times10^7$ $M^{-1}s^{-1}$, respectively (Buxton et al., 1988; Moussavi et al., 2018). The experiment was conducted using the following conditions: initial pH = 10.4, $[CN^-]$ = 4 mM, borate buffer = 0.03 M, [PDS] = 10 mM, $[Cu^{2+}]$ = 1 mM. The result is shown in Figure 12. It was found that methanol had a slight inhibitory impact on cyanide removal initially (< 5 min) but had no impact on the final removal. It was speculated that methanol might react with OH · to form other radicals, such as $CH_2OH$ · and $CH_3O$ · to improve cyanide removal (Buxton et al., 1988) Hence, OH · and $SO_4^-$ · were involved in the reaction, but which radical was the main contributor on cyanide removal could not be revealed.

Radical probe experiments using 4-chlorbenzoic acid (pCBA) and benzoic acid (BA) as the probe compounds ($k_{pCBA/OH\cdot} = 5.2\times10^9$ $M^{-1}s^{-1}$, $k_{pCBA/SO_4^-\cdot} = 3.6\times10^8$ $M^{-1}s^{-1}$, $k_{BA/OH\cdot} = 5.9\times10^9$ $M^{-1}s^{-1}$, $k_{BA/SO_4^-\cdot} = 1.2\times10^9$ $M^{-1}s^{-1}$) were conducted to investigate the contribution of OH · and $SO_4^-$ · on cyanide removal in this system (Pi et al., 2005; Guan et al., 2011; Lutze et al., 2015). The rate constant of pCBA and BA reactions with OH · are almost the same, while $k_{pCBA/SO_4^-\cdot}$ is three times smaller than $k_{BA/SO_4^-\cdot}$. Thus, pCBA



doi:10.6342/NTU202202427

tends to react with OH · compared to $SO_4^-$ · . The results showed that pCBA removal efficiency was much lower than BA, indicating that OH · and $SO_4^-$ · contributed to the removal of cyanide in this system. After 20 min of reaction, the removal efficiency of pCBA and BA were about 33% and 67%, respectively (Figure 13). Additional experiments were conducted with cyanide to confirm the contribution of OH · and $SO_4^-$ · on cyanide removal. The result is shown in Figure 14. Compared with the group added pCBA, the inhibition effect of cyanide removal was higher in the group added BA within 10 min but had no impact on the final removal. It was suggested that OH · and $SO_4^-$ · had some contribution on cyanide removal in $Cu^{2+}$ activate PDS system, but there still had some other reactive species that may improve cyanide removal.

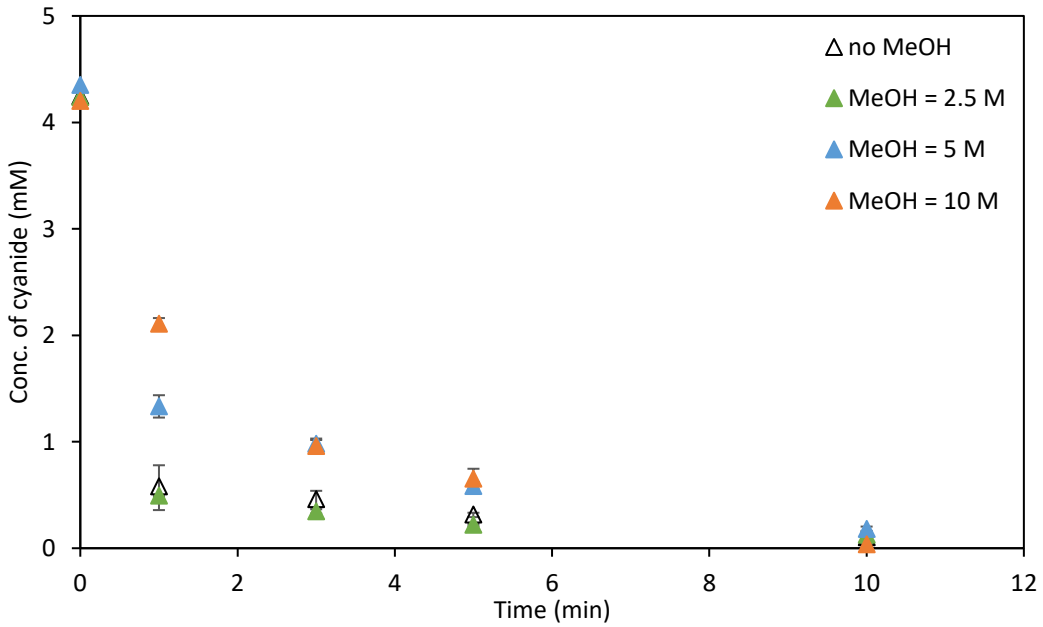


Figure 12. Influence of methanol on cyanide removal. (Experimental condition: initial pH = 10.4, $[CN^-]$ = 4 mM, borate buffer = 0.03 M, [PDS] = 10 mM, $[Cu^{2+}]$ = 1 mM)



doi:10.6342/NTU202202427

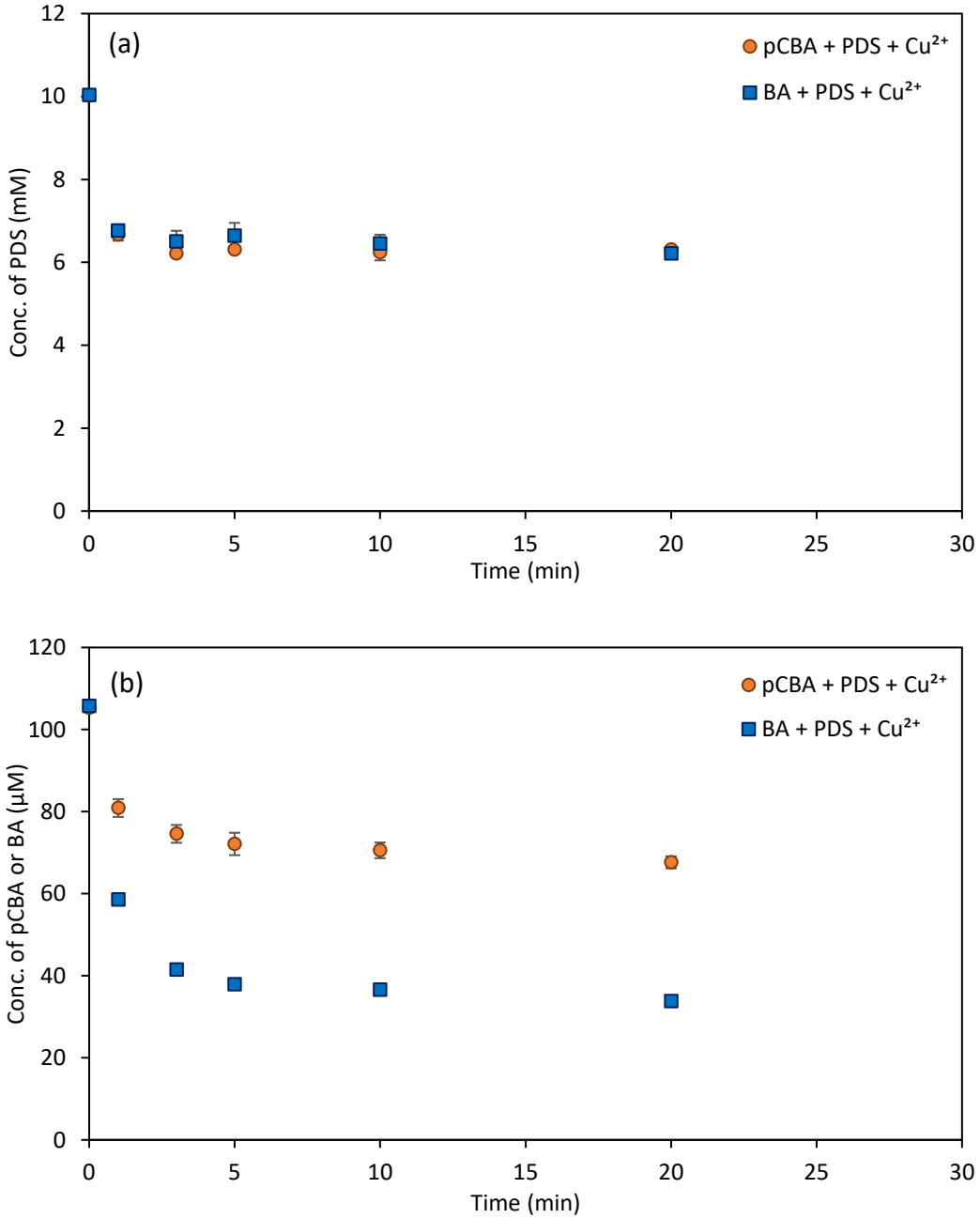


Figure 13. pCBA and BA radical probe experiments (a) PDS consumption and (b) the pCBA or BA degradation (Experimental condition: initial pH = 10.2, borate buffer = 0.03 M, [PDS] = 10 mM, [$Cu^{2+}$] = 1 mM, [pCBA]or [BA] = 100 μM)



doi:10.6342/NTU202202427

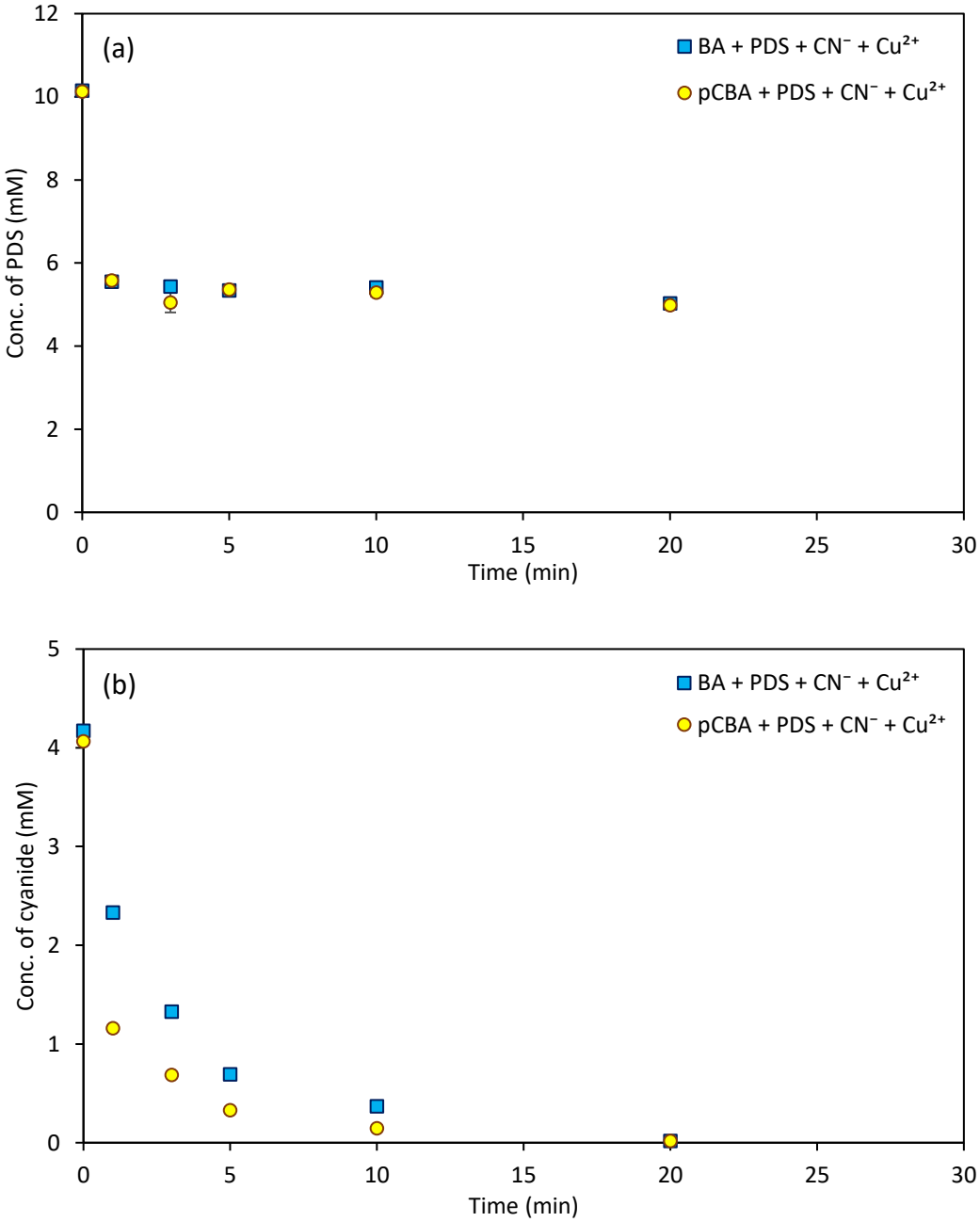


Figure 14. pCBA and BA radical probe experiments (a) PDS consumption and (b) cyanide removal (Experimental condition: initial pH = 9.99, borate buffer = 0.03 M, [PDS] = 10 mM, $[CN^-]$ = 4 mM, $[Cu^{2+}]$ = 1 mM, [pCBA]or [BA] = 100 μM)



doi:10.6342/NTU202202427

## 4.4 Characterization of by-products formed in cyanide oxidation by activated PDS

The by-products of cyanide oxidation by activated PDS, including $OCN^-$, $NH_3$-N, $NO_2^-$, and $NO_3^-$ were measured to better characterize the process. Figure 15 shows the byproducts formed in the following experimental condition without (PDS/$CN^-$) and with the addition of 1 mM $Cu^{2+}$ (PDS/$CN^-$/$Cu^{2+}$): initial pH = 10.2, [$CN^-$] = 4 mM, borate buffer = 0.03 M, [PDS] = 10 mM.

In the absence of $Cu^{2+}$ (Figure 15 (a)), cyanide removal in the end of the experiment was around 15% and the $OCN^-$ concentration increased to 0.24 mM. The concentrations of nitrite and nitrate were very low. Ammonia was not observed in the experiment.

In the presence of 1 mM $Cu^{2+}$ (Figure 15 (b)), $OCN^-$ concentration continued to increase to 3.5 mM and cyanide continued to decrease to almost zero after 20 min. $OCN^-$ was the dominant by-product formed in this PDS/$CN^-$/$Cu^{2+}$ system. $NO_2^-$ was formed by the oxidation of $OCN^-$ and its concentration was about 0.4 mM after 20 min. The concentration of $NO_3^-$ was very low and ammonia was not observed in this system.



doi:10.6342/NTU202202427

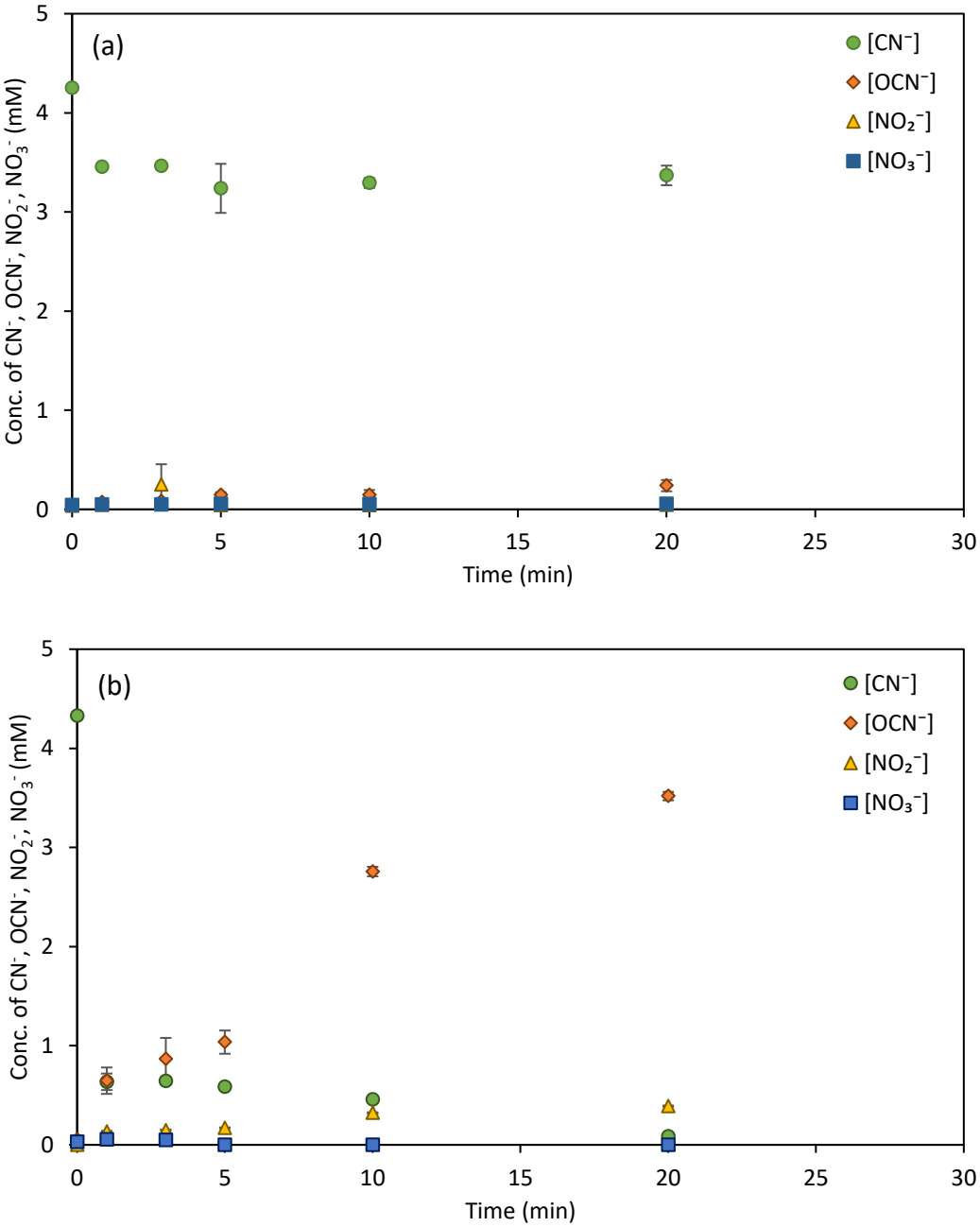


Figure 15. By-products analysis in cyanide oxidation process: (a) PDS/$CN^-$ system (b) PDS/$CN^-$/$Cu^{2+}$ system. (Experimental condition: initial pH = 10.2, [$CN^-$] = 4 mM, borate buffer = 0.03 M, [PDS] = 10 mM, [$Cu^{2+}$] = 1 mM)



doi:10.6342/NTU202202427

Figure 16 shows the nitrogen balance using the residual $CN^-$ concentration and all nitrogen-containing by-products as a function of time. In the PDS/$CN^-$ system, the sum of $CN^-$, $OCN^-$, $NO_2^-$, and $NO_3^-$ after 20 min was about 3.7 mM, in which about 0.88 mM of $CN^-$ was removed and 0.24 mM of $OCN^-$ and minimal $NO_2^-$ and $NO_3^-$ were produced, suggesting that there was a 0.55 mM of nitrogen loss. In the PDS/$CN^-$/$Cu^{2+}$ system, the sum of $CN^-$, $OCN^-$, $NO_2^-$, and $NO_3^-$ after 5 min of the reaction was about 1.8 mM, while about 3.7 mM of $CN^-$ was removed and 1.0 mM of $OCN^-$ was produced, suggesting that a loss of 0.33 mM of nitrogen and other unmeasured by-products was produced during the reaction. Since the $CN^-$ concentration gradually decreased with time and the total concentration of all by-products was approximately equal to the initial cyanide concentration and dominated by $OCN^-$ after 20 min, it was likely that a unmeasured by-product was formed before $OCN^-$ and later converted to $OCN^-$ as the reaction proceeded. According to Equations ( 6) and ( 7), the C(OH)=N· radical could be the unmeasured by-product.



doi:10.6342/NTU202202427

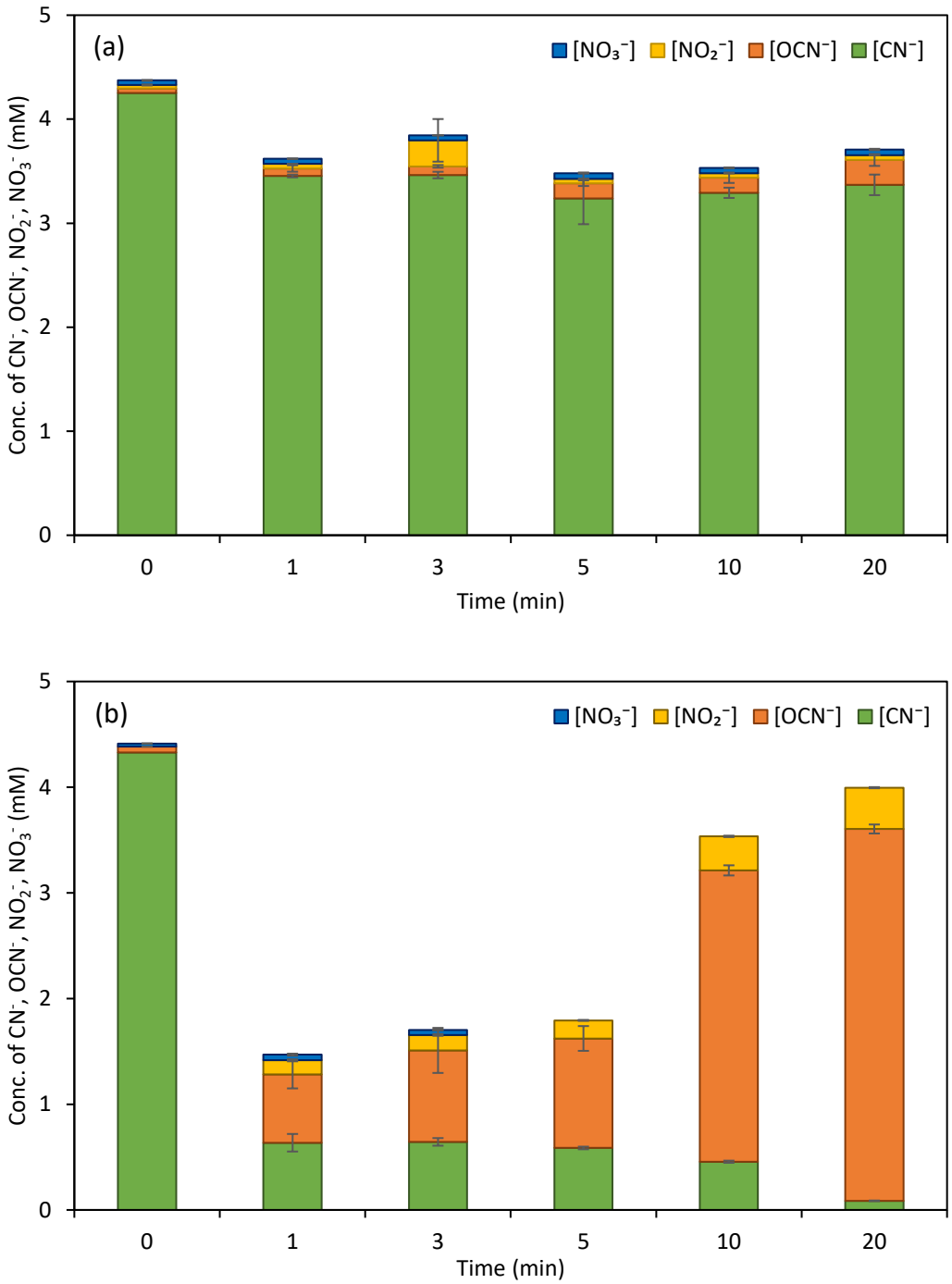


Figure 16. Summary of by-products analysis in cyanide oxidation process: (a) PDS/$CN^-$ system (b) PDS/$CN^-$/$Cu^{2+}$. (Experimental condition: initial pH = 10.2, [$CN^-$] = 4 mM, borate buffer = 0.03 M, [PDS] = 10 mM, [$Cu^{2+}$] = 1 mM)



doi:10.6342/NTU202202427

## 4.5 EPR experiments

EPR experiments can be used to further confirm the generation of OH・and $SO_4^-$・in the $Cu^{2+}$-activated PDS oxidation. DMPO was used as a spin trap chemical to form adducts with the radicals.

The EPR spectra obtained from different experimental conditions are shown in Figure 17. In DI water, no radical signal was found. In the presence of borate buffer at pH = 10.2, there was a small signal of DMPO-OH・due to the alkaline condition (Bernofsky et al., 1990). In the group of borate buffer + $Cu^{2+}$, there was a small signal of DMPO-OH・because the combination of $Cu^{2+}$ and DMPO can polarize the double bond of DMPO and promote the formation of DMPO-OH・(Walger et al., 2021). Furthermore, the signals of DMPO-R and triplet radical were found in this group due to the DMPO decomposition in the presence of $Cu^{2+}$ (Walger et al., 2021). For the group of borate buffer + PDS, a small signal of DMPO-OH・and a tiny signal of DMPO-$SO_4^-$・were observed due to the alkaline activation of PDS. One the other hand, a stronger signal of DMPO-$SO_4^-$・was observed in the group of borate buffer + PDS + $Cu^{2+}$, which verified that PDS can be activated by $Cu^{2+}$ to form OH・and $SO_4^-$・. However, the strongest signal was detected in the group of borate buffer + $CN^-$ + PDS + $Cu^{2+}$. It was speculated that DMPO might react with other radicals (C(OH)=N・) generated during cyanide oxidation.



doi:10.6342/NTU202202427

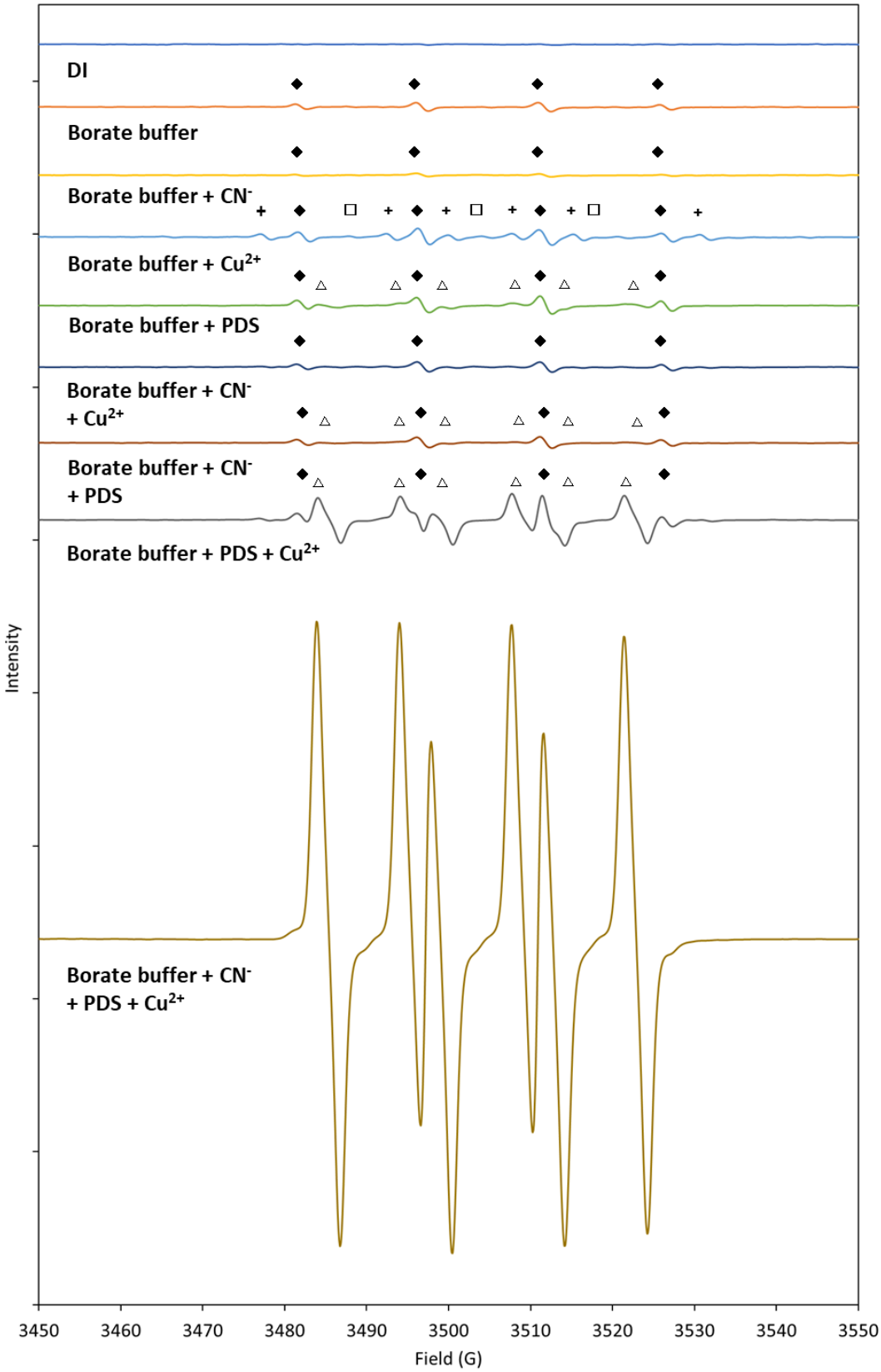


Figure 17. EPR spectra of PDS/$Cu^{2+}$/$CN^-$ system. (Experimental condition: borate buffer = 0.03 M, [$CN^-$] = 4 mM, [PDS] = 10 mM, [$Cu^{2+}$] = 1 mM, [DMPO] = 1 M, ◆: DMPO-OH・, △: DMPO-$SO_4^-$・, ┼: DMPO-R, □: triplet radical)



doi:10.6342/NTU202202427

## 4.6 Application of PDS oxidation process in the treatment of cyanide-containing electroplating wastewater

The real cyanide wastewater sample was obtained from an electroplating factory, which uses silver cyanide complexes to plat copper objects. Since the electroplating process includes degreasing, pickling and electroplating, wastewater contained high concentrations of cyanide, silver, copper, and other metals ions and anions. The characteristic of real wastewater was as follows: pH = 11.4, conductivity = 2.99 mS/cm, total cyanide = 507 mg/L, concentrations of other elements are shown in Table 13.

Table 13. Composition of cyanide electroplating wastewater.

| Element | Initial concentration (mg/L) | Final concentration after 40 mM PDS oxidation process (mg/L) |
|---|---|---|
| Ag | 39.8 | 34.5 |
| Cd | 0.079 | ND |
| Cr | 0.110 | ND |
| Cu | 241 | 206 |
| Fe | 0.317 | 0.154 |
| Mn | 0.106 | ND |
| Ni | 3.16 | 2.24 |
| Pb | 0.357 | ND |
| Zn | 13.0 | 7.55 |
| $F^-$ | 90.1 | 86.3 |
| $Cl^-$ | 14.8 | 16.1 |
| $NO_2^-$ | 2.11 | 263 |
| $NO_3^-$ | 2.64 | 6.03 |
| $PO_4^{3-}$ | ND | ND |
| $SO_4^{2-}$ | 36.9 | 40.2 |



doi:10.6342/NTU202202427

The cyanide removal experiments were carried out using 10, 25, and 40 mM PDS corresponding to the [PDS]/[$CN^-$] molar ratio of 0.5, 1.25, 2, respectively. The concentrations of cyanide, cyanate, ammonia, nitrite, nitrate, and PDS were measured as a function of time. Figure 18 shows the results of 10 mM PDS without pH adjustment. The removal of cyanide was observed within 1 min and no significant change thereafter. PDS was almost completely consumed after 5 min of reaction, suggesting that the amount of PDS was insufficient to completely cyanide in this electroplating wastewater. The cyanide removal efficiency was about 50% and 1.4 mM of nitrite was produced. However, the by-product analysis in electroplating wastewater was difficult to compare with the results in Section 4.3, because different compositions of PDS, cyanide and copper ions might lead to different cyanide conversion. Since 25 mM PDS had 2.9 mM of residual cyanide after 20 min, an attempt was made to remove cyanide at least 99.8% from the wastewater by the addition of 40 mM PDS to achieve an effluent standard of 1 mg/L total cyanide.

Figure 19 shows the results of 40 mM PDS and pH control at about 10.5 during the reaction by using 6 mM NaOH. The concentration of cyanide decreased and that of nitrite increased over time. In the end of the experiment, the residual PDS was 3.19 mM, the concentration of nitrite was 5.72 mM, and the residual cyanide was 0.6 mg/L, which met the water quality standard of electroplating effluents in Taiwan. The by-products



doi:10.6342/NTU202202427

measurement showed that the sum of $CN^-$, $OCN^-$, $NH_3$-N, $NO_2^-$, and $NO_3^-$ was about 6 mM, suggesting that nitrogen gas may be generated during the reaction (Figure 19(b)). In addition, the metal ion measurements indicated that 35 mg/L of copper was consumed and the concentration of some metal including iron, lead, and zinc decreased after 20 min of reaction (Table 13), indicating that in additional to cyanide, the process can simultaneously remove some metals from the electroplating wastewater. A brown precipitate was found in the end of the experiments. In order to prevent the composition of the membrane filter from interfering the determination of the precipitate composition, the SEM-EDS images and element composition of membrane filter and membrane filter with precipitate are observed, as shown in Table 14 and Figure 20. C, N and O were the main constituents of membrane filter, while Na, S, K, Ca, Fe, Cu, and Ag were found in the presence of precipitates. The results showed that metals may participate in the PDS activation process or become hydroxides under alkaline condition, and then form precipitates after the reaction.



doi:10.6342/NTU202202427

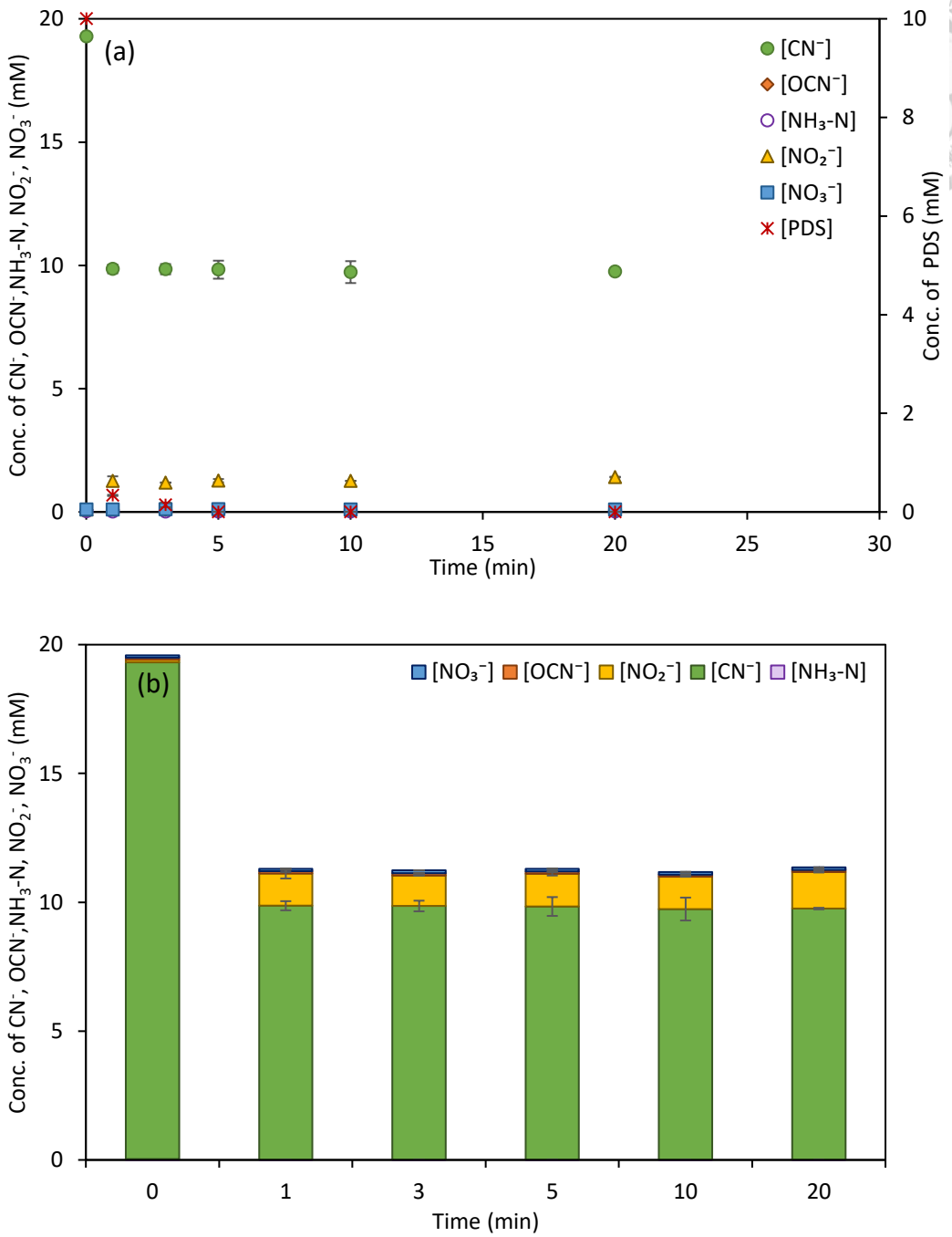


Figure 18. Electroplating wastewater treatment in PDS oxidation process without pH control. (Experimental condition: initial pH = 11.4, final pH = 8.9, [PDS] = 10 mM)



doi:10.6342/NTU202202427

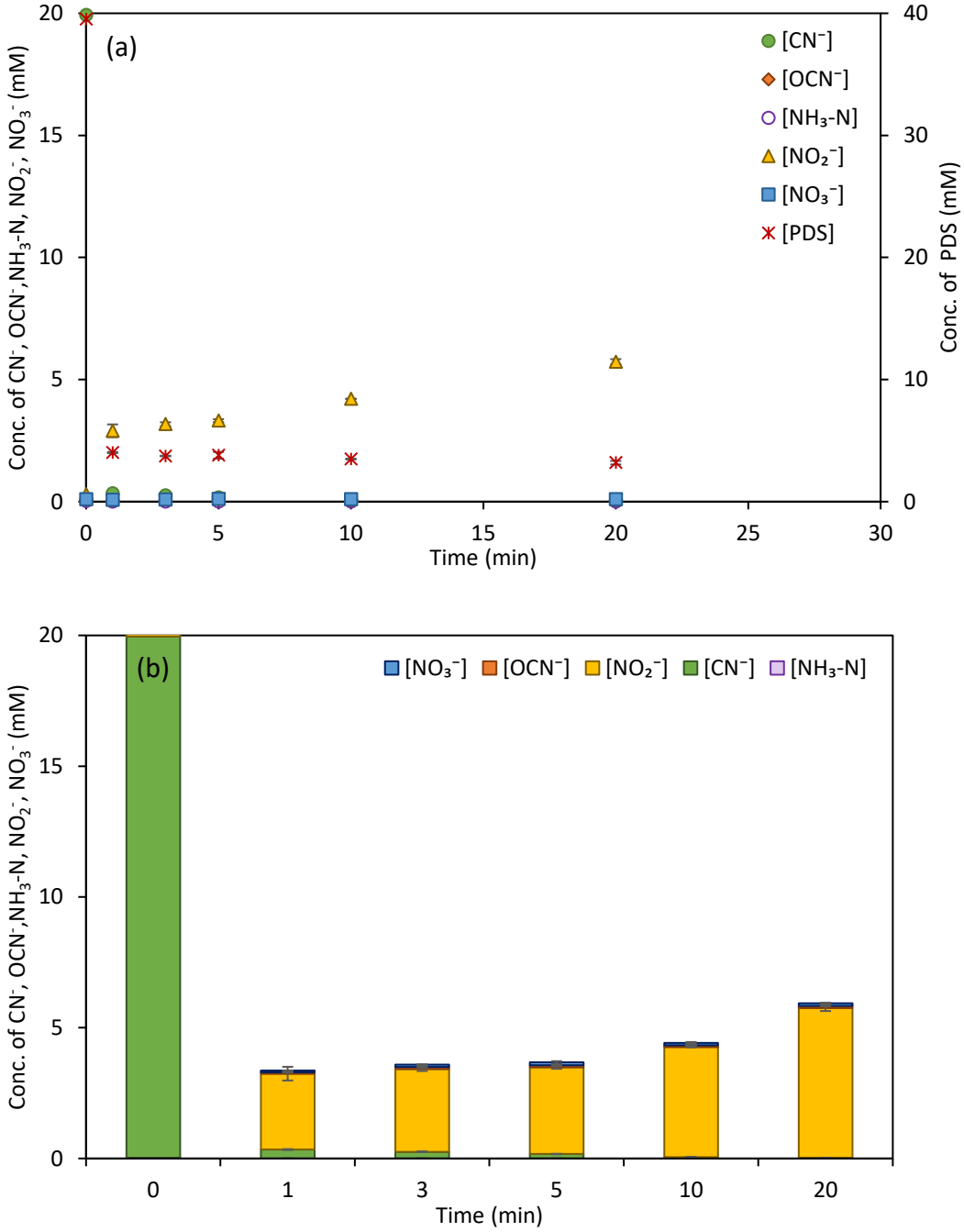


Figure 19. Electroplating wastewater treatment in PDS oxidation process with pH control by using 6 M NaOH. (Experimental condition: initial pH = 10.8, final pH = 10.3, [PDS] = 40 mM)



doi:10.6342/NTU202202427

Table 14. Element compositions (%) of membrane filter and membrane filter with precipitate determined by SEM-EDS.

| Element | Membrane filter | Membrane filter with Precipitate |
|---|---|---|
| C | 41.9 | 44.3 |
| N | 7.82 | 13.1 |
| O | 50.3 | 34.0 |
| Na | - | 2.55 |
| S | - | 1.05 |
| K | - | 0.26 |
| Ca | - | 0.18 |
| Fe | - | 1.50 |
| Cu | - | 1.26 |
| Ag | - | 1.80 |

Figure 20. SEM-EDS of (a) membrane filter and (b) membrane filter with precipitate.

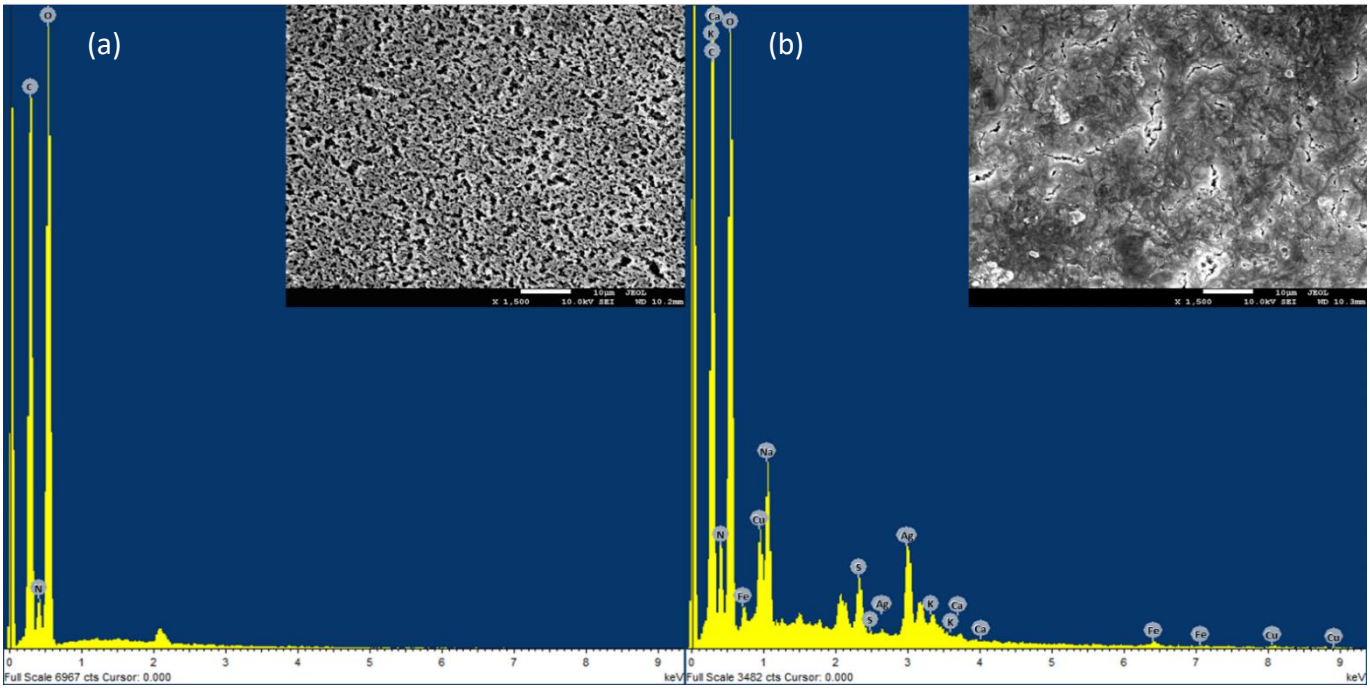




doi:10.6342/NTU202202427

# Chapter 5 Conclusions and Recommendations

## 5.1 Conclusions

The removal of cyanide by persulfate oxidation process was investigated in the synthetic solution and real wastewater. The effects of water quality parameters on cyanide removal were evaluated. The following conclusions could be obtained from this research:

1. The molar ratio of [PDS]/[$CN^-$] should be greater than 1:1 to remove cyanide effectively.
2. The presence of anions did not affect the removal efficiency of cyanide. Common metal ions present in electroplating wastewater showed the following trends in activating PDS for cyanide removal: $Cu^{2+} > Zn^{2+} > Fe^{2+} > Ni^{2+}$.
3. Cyanate and nitrite were the main by-products formed from cyanide removal by the PDS oxidation process.
4. Based on radical scavenging experiments and EPR spectra results, copper ion could activate PDS to generate hydroxyl radicals and sulfate radicals.
5. Activation of PDS by copper ion could be a promising process for efficient cyanide removal in real electroplating wastewater.



doi:10.6342/NTU202202427

## 5.2 Recommendations

1. In this study, the influences of cyanide concentration, PDS concentration and copper concentration on cyanide removal and PDS consumption were evaluated. However, the reaction rates were too fast to use kinetic models to simulate the reaction kinetics. A stop flow system can be used to study the fast kinetics in the future study.
2. Three common metal ions in electroplating wastewater were selected to add into synthetic cyanide solution individually, but multiple metal ions may co-exist in real electroplating wastewater. Therefore, further studies can conduct in the presence of different metal ions simultaneously to evaluate cyanide removal.
3. PDS oxidation process can be carried out in a continuous flow reactor to simulate the real treatment process of cyanide removal in the electroplating plant.



doi:10.6342/NTU202202427

# Reference

Adachi, A., Nojima, S., Hagiwaras, Y., Hamamoto, M. and Kobayashi, T. (1991) Studies on the oxidative decomposition of cyanide ion by potassium permanganate. *Environmental Technology,* 12**,** 93-96.

Adams, M. D. (2013) Impact of recycling cyanide and its reaction products on upstream unit operations. *Minerals Engineering,* 53**,** 241-255.

Anipsitakis, G. P. and Dionysiou, D. D. (2003) Degradation of organic contaminants in water with sulfate radicals generated by the conjunction of peroxymonosulfate with cobalt. *Environmental Science & Technology,* 37**,** 4790-4797.

Anipsitakis, G. P. and Dionysiou, D. D. (2004) Radical generation by the interaction of transition metals with common oxidants. *Environmental Science & Technology,* 38**,** 3705-3712.

APHA, AWWA and WEF (2017) Standard methods for the examination of water and wastewater, 23rd.

Behnami, A., Croué, J.-P., Aghayani, E. and Pourakbar, M. (2021) A catalytic ozonation process using MgO/persulfate for degradation of cyanide in industrial wastewater: mechanistic interpretation, kinetics and by-products. *RSC Advances,* 11**,** 36965-36977.

Bernofsky, C., Bandara, B. M. R. and Hinojosa, O. (1990) Electron spin resonance



doi:10.6342/NTU202202427

studies of the reaction of hypochlorite with 5,5-dimethyl-1-pyrroline-N-oxide. *Free Radical Biology and Medicine,* 8**,** 231-239.

Botz, M. M., Mudder, T. I. and Akcil, A. U. (2016) Chapter 35 - Cyanide Treatment: Physical, Chemical, and Biological Processes. In *Gold Ore Processing (Second Edition),* ed. M. D. Adams, 619-645. Elsevier.

Branch, S. W. (1993) Cyanide detoxification: INCO sulfur dioxide/air process.

Budaev, S. L., Batoeva, A. A. and Tsybikova, B. A. (2015) Degradation of thiocyanate in aqueous solution by persulfate activated ferric ion. *Minerals Engineering,* 81**,** 88-95.

Buxton, G. V., Greenstock, C. L., Helman, W. P. and Ross, A. B. (1988) Critical review of rate constants for reactions of hydrated electrons, hydrogen atoms and hydroxyl radicals in aqueous solution. *J. Phys. Chem. Ref. Data,* 17**,** 886.

Castilla-Acevedo, S. F., Betancourt-Buitrago, L. A., Dionysiou, D. D. and Machuca-Martínez, F. (2020) Ultraviolet light-mediated activation of persulfate for the degradation of cobalt cyanocomplexes. *Journal of Hazardous Materials,* 392**,** 122389.

Chegini, Z. G., Hassani, H., Torabian, A. and Borghei, S. M. (2020) Enhancement of PMS activation in an UV/ozone process for cyanide degradation: a comprehensive study. *Pigment & Resin Technology*, 6.



doi:10.6342/NTU202202427

Chen, F., Zhao, X., Liu, H. and Qu, J. (2014) Reaction of Cu $(CN)_3^{2-}$ with $H_2O_2$ in water under alkaline conditions: cyanide oxidation, $Cu^+/Cu^{2+}$ catalysis and $H_2O_2$ decomposition. *Applied Catalysis B: Environmental,* 158**,** 85-90.

Chen, J., Zhou, X., Sun, P., Zhang, Y. and Huang, C.-H. (2019) Complexation enhances Cu(II)-activated peroxydisulfate: A novel activation mechanism and Cu(III) contribution. *Environmental Science & Technology,* 53**,** 11774-11782.

Cheng, C.-F., Lin, H. H.-H., Tung, H.-H. and Lin, A. Y.-C. (2022) Enhanced solar photodegradation of a plasmid-encoded extracellular antibiotic resistance gene in the presence of free chlorine. *Journal of Environmental Chemical Engineering,* 10**,** 106984.

Cui, M., Jang, M., Lee, S. and Khim, J. (2012) Sonochemical oxidation of cyanide using potassium peroxydisulfate as an oxidizing agent. *Japanese Journal of Applied Physics,* 51**,** 07GD13.

Dash, R. R., Balomajumder, C. and Kumar, A. (2009) Removal of cyanide from water and wastewater using granular activated carbon. *Chemical Engineering Journal,* 146**,** 408-413.

Devi, P., Das, U. and Dalai, A. K. (2016) In-situ chemical oxidation: Principle and applications of peroxide and persulfate treatments in wastewater systems. *Science of The Total Environment,* 571**,** 643-657.



doi:10.6342/NTU202202427

Devuyst, E., Conard, B., Vergunst, R. and Tandi, B. (1989) A cyanide removal process using sulfur dioxide and air. *JOM,* 41**,** 43-45.

Ding, Y., Fu, L., Peng, X., Lei, M., Wang, C. and Jiang, J. (2022) Copper catalysts for radical and nonradical persulfate based advanced oxidation processes: Certainties and uncertainties. *Chemical Engineering Journal,* 427**,** 131776.

EPA, U. S. (1979) Environmental pollution control alternatives economics of wastewater treatment alternatives for the electroplating industry.

Furman, O. S., Teel, A. L. and Watts, R. J. (2010) Mechanism of base activation of persulfate. *Environmental Science & Technology,* 44**,** 6423-6428.

Gokulakrishnan, S., Mohammed, A. and Prakash, H. (2016) Determination of persulphates using N, N-diethyl-p-phenylenediamine as colorimetric reagent: Oxidative coloration and degradation of the reagent without bactericidal effect in water. *Chemical Engineering Journal,* 286**,** 223-231.

Guan, Y.-H., Ma, J., Li, X.-C., Fang, J.-Y. and Chen, L.-W. (2011) Influence of pH on the formation of sulfate and hydroxyl radicals in the UV/peroxymonosulfate system. *Environmental Science & Technology,* 45**,** 9308-9314.

Guerra-Rodríguez, S., Rodríguez, E., Singh, D. N. and Rodríguez-Chueca, J. (2018) Assessment of sulfate radical-based advanced oxidation processes for water and wastewater treatment: a review. *Water,* 10**,** 1828.



doi:10.6342/NTU202202427

Gurbuz, F., Ciftci, H. and Akcil, A. (2009) Biodegradation of cyanide containing effluents by Scenedesmus obliquus. *Journal of Hazardous Materials,* 162**,** 74-79.

Industrial Development Bureau, M. O. E. A. (2002) 電鍍業資源化應用技術手冊.

Johnson, C. A. (2015) The fate of cyanide in leach wastes at gold mines: An environmental perspective. *Applied Geochemistry,* 57**,** 194-205.

Kim, T.-K., Kim, T., Jo, A., Park, S., Choi, K. and Zoh, K.-D. (2018) Degradation mechanism of cyanide in water using a UV-LED/$H_2O_2$/$Cu^{2+}$ system. *Chemosphere,* 208**,** 441-449.

Kim, Y. J., Qureshi, T. and Min, K. S. (2003) Application of advanced oxidation processes for the treatment of cyanide containing effluent. *Environmental technology,* 24**,** 1269-1276.

Lau, T. K., Chu, W. and Graham, N. J. D. (2007) The aqueous degradation of butylated hydroxyanisole by UV/$S_2O_8^{2-}$: Study of reaction mechanisms via dimerization and mineralization. *Environmental Science & Technology,* 41**,** 613-619.

Lutze, H. V., Kerlin, N. and Schmidt, T. C. (2015) Sulfate radical-based water treatment in presence of chloride: formation of chlorate, inter-conversion of sulfate radicals into hydroxyl radicals and influence of bicarbonate. *Water research,* 72**,** 349-360.



doi:10.6342/NTU202202427

Matzek, L. W. and Carter, K. E. (2016) Activated persulfate for organic chemical degradation: A review. *Chemosphere,* 151**,** 178-188.

Moussavi, G., Pourakbar, M., Aghayani, E. and Mahdavianpour, M. (2018) Investigating the aerated VUV/PS process simultaneously generating hydroxyl and sulfate radicals for the oxidation of cyanide in aqueous solution and industrial wastewater. *Chemical Engineering Journal,* 350**,** 673-680.

Moussavi, G., Pourakbar, M., Aghayani, E., Mahdavianpour, M. and Shekoohyian, S. (2016) Comparing the efficacy of VUV and UVC/$S_2O_8^{2-}$ advanced oxidation processes for degradation and mineralization of cyanide in wastewater. *Chemical Engineering Journal,* 294**,** 273-280.

National Institute of Environmental Analysis, NIEA. (2011) 環境檢驗所廢水處理流程說明.

Nava, F., Uribe, A. and Pérez, R. (2003) Use of ozone in the treatment of cyanide containing effluents. *European Journal of Mineral Processing & Environmental Protection,* 3.

Ordiales, M., Fernandez, D., Verdeja, L. F. and Sancho, J. (2015) Potassium permanganate as an alternative for gold mining wastewater treatment. *Jom,* 67**,** 1975-1985.

Pérez-Cid, B., Calvar, S., Moldes, A. B. and Manuel Cruz, J. (2020) Effective removal



doi:10.6342/NTU202202427

of cyanide and heavy metals from an industrial electroplating stream using calcium alginate hydrogels. *Molecules,* 25**,** 5183.

Parga, J. R., Shukla, S. S. and Carrillo-Pedroza, F. R. (2003) Destruction of cyanide waste solutions using chlorine dioxide, ozone and titania sol. *Waste Management,* 23**,** 183-191.

Pi, Y., Schumacher, J. and Jekel, M. (2005) The use of para-chlorobenzoic acid (pCBA) as an ozone/hydroxyl radical probe compound. *Ozone: Science and Engineering,* 27**,** 431-436.

Popova, T. and Aksenova, N. (2003) Complexes of copper in unstable oxidation states. *Russian Journal of Coordination Chemistry,* 29**,** 743-765.

Pueyo, N., Miguel, N., Ovelleiro, J. L. and Ormad, M. P. (2016) Limitations of the removal of cyanide from coking wastewater by ozonation and by the hydrogen peroxide-ozone process. *Water Science and Technology,* 74**,** 482-490.

Sarla, M., Pandit, M., Tyagi, D. and Kapoor, J. (2004) Oxidation of cyanide in aqueous solution by chemical and photochemical process. *Journal of Hazardous Materials,* 116**,** 49-56.

Satizabal-Gómez, V., Collazos-Botero, M. A., Serna-Galvis, E. A., Torres-Palma, R. A., Bravo-Suárez, J. J., Machuca-Martínez, F. and Castilla-Acevedo, S. F. (2021) Effect of the presence of inorganic ions and operational parameters on free



doi:10.6342/NTU202202427

cyanide degradation by ultraviolet C activation of persulfate in synthetic mining wastewater. *Minerals Engineering,* 170**,** 107031.

Teixeira, L. A. C., Andia, J. P. M., Yokoyama, L., da Fonseca Araújo, F. V. and Sarmiento, C. M. (2013) Oxidation of cyanide in effluents by Caro's Acid. *Minerals Engineering,* 45**,** 81-87.

Walger, E., Marlin, N., Mortha, G., Molton, F. and Duboc, C. (2021) Hydroxyl radical generation by the $H_2O_2/Cu^{2+}$/phenanthroline system under both neutral and alkaline conditions: an EPR/Spin-Trapping Investigation. *Applied Sciences,* 11**,** 687.

Wang, J. and Wang, S. (2018) Activation of persulfate (PS) and peroxymonosulfate (PMS) and application for the degradation of emerging contaminants. *Chemical Engineering Journal,* 334**,** 1502-1517.

Wei, Y., Chen, S., Ren, T., Chen, L., Liu, Y., Gao, J. and Li, Y. (2022) Effectiveness and mechanism of cyanide remediation from contaminated soils using thermally activated persulfate. *Chemosphere,* 292**,** 133463.

Yang, W., Liu, G., Chen, Y., Miao, D., Wei, Q., Li, H., Ma, L., Zhou, K., Liu, L. and Yu, Z. (2020) Persulfate enhanced electrochemical oxidation of highly toxic cyanide-containing organic wastewater using boron-doped diamond anode. *Chemosphere,* 252**,** 126499.



doi:10.6342/NTU202202427

Zhang, J., Liu, L., Liang, Y., Zhou, J., Xu, Y., Ruan, X., Lu, Y., Xu, Z. and Qian, G. (2015) Enhanced precipitation of cyanide from electroplating wastewater via self-assembly of bimetal cyanide complex. *Separation and Purification Technology,* 150**,** 179-185.

Zheng, X., Niu, X., Zhang, D., Lv, M., Ye, X., Ma, J., Lin, Z. and Fu, M. (2022) Metal-based catalysts for persulfate and peroxymonosulfate activation in heterogeneous ways: A review. *Chemical Engineering Journal,* 429**,** 132323.

李依釗 (2016) 廢水處理廠代操作策略暨功能評估.



doi:10.6342/NTU202202427